People's Democratic Republic of Algeria Ministry of Higher
Education and Scientific Research

University M'Hamed BOUGARA – Boumerdes

Institute of Electrical and Electronic Engineering

Department of Electronics

Final Year Project Report Presented in Partial Fulfilment of the Requirements for the Degree of

MASTER

In **Electrical and Electronic Engineering**

Option: **Telecommunications**

Title:

Design and analysis of a compact Triple-band Antenna for WLAN/WiMAX applications

Presented by:

Mohamed El Amine ZEBOUDJ

Supervisor:

Dr . K. DJAFRI

INTROUCTION

With the rapid growth of the wireless mobile communication technology, and by the emerging of many new standards for wireless communications including RFID, Wi-Fi, fourth generation/Long-Term Evolution (LTE), Worldwide Interoperability for Microwave Access (WiMAX) which are working in the frequency range of 700 MHz to 6 GHz, the main limitation of microstrip antenna is its physical size. For this reason, much effort has been devoted to the development of compact multiband antennas. Therefore, new techniques for designing compact and multiband antenna need to be investigated, which is the key motivation of this thesis work **[1].**

The type of the antenna we have discussed and worked on in this project is a triple band microstrip patch. The patch geometry has been chosen carefully to cover specifically 2.4 / 5.5 WLAN and 3.5 WiMAX allotted bands. The proposed structure is based on an adequate combination of two octagonal rings. The inner sides of outer radiating ring have been attached to eight octagonal shaped branches to obtain frequency-tunable antenna. The resulted design operates at three bands over a frequency range from 2 to 6 GHz with a compact size of 25.5 x 20 mm^2 and its radio electric parameters have been discussed in detail.

This report includes three main chapters and it is organized as follows:

Chapter 1 presents an overview on Microstrip Patch Antennas including basic parameters, feeding techniques, as well as advantages and disadvantages.

Chapter 2 gives the detailed procedure to design triple band antenna starting from a simple triangular shaped patch antenna and ending with interconnected dual octagonal rings geometry. Various intermediate are considered and theirs return losses over the considered range of frequency are simulated and analyzed.

In Chapter 3, the detailed analysis of the proposed structure is provided. Besides, an extensive parametric study is carried to have better understanding of the operating mechanism.

A conclusion is presented at the end of the report.

DEDICATIONS

I would like to dedicate my work: to my beloved parents for their enthusiastic caring throughout my life. Thanks a lot for the support you have given me throughout my life to my loving brothers and sisters.

ACKNOWLEDGEMENTS

I give thanks to Allah for having made it possible for me to finish this work. Thereafter, I would like to take this opportunity to express deep and sincere gratitude to my Supervisor Professor ***DJAFRI.K*** *for her supervision, advice and guidance from the very early stage of this project.*

I'm also so thankful to my parents, my brothers, my sisters, my friends whose helps and support, Thanks you all.

ABSTRACT

In this work, a reduced size tri-band monopole antenna has been designed, fabricated and tested. This is achieved by using a new geometrical patch based on two interconnected concentric octagonal rings. In order to tune independently the resonant frequencies, the outer ring has been attached to eight octagonal patches. The final antenna has a compact size ($20 \times 25.5 \times 1.63$ $mm^{3)}$, planar, simple design and low cost to be manufactured. Moreover, the proposed antenna operates in three useful bands covering the 2.4-GHz WLAN, 3.5-GHz WiMAX and 5.5-GHz WLAN simultaneously, has good stable omnidirectional radiation patterns, and the peak gain over the operating bands are 1.82, 1.91 and 3.94dB, respectively.

LIST OF SYMBOLS

ϵ_r	Relative permittivity
Z_c	Characteristic impedance
k	Wave number
k_0	Free space wave number
(r, θ, ϕ)	Spherical coordinate system
U_0	Radiation intensity of an isotropic antenna
$Umax$	Maximum radiation intensity
D_0	Maximum Directivity
P_{rad}	Radiated power
$E_{r,\theta,\phi}$	Electric field intensity
$E_{t,\theta,\phi}$	Total electric field intensity
λ	Wavelength.
λ_0	Free-space wavelength.
R_r	Radiation resistance
R_m	Material losses resistance
η_s	Efficiency of the system
η_a	Efficiency of the antenna
Q_s	System quality factor
Q_a	Antenna quality factor
Q_m	Matching network quality factor
f_r	resonant frequency
c	Speed of light in free space
h	Substrate height
W	Patch width
t	thickness of metallic strip
L	Inductance
L_{eff}	Effective length
S_{11}	Return loss
f_h	upper cut off frequency

f_l	lower cut off frequency
f_{mn}	The resonant frequency
f_c	Central frequency of the band

LIST OF ABBREVIATION

WLAN	Wireless Local Area Network
Wi-Fi	Wireless Fidelity
RFID	Radio Frequency Identification
TV	Television
LTE	Long-Term Evolution
WiMAX	Worldwide Interoperability for Microwave Access
EM	Electromagnetic
DMS	Defected Microstrip Structure
DRA	Dielectric Resonator Antenna
TLM	Transmission line method
CM	Cavity model
VSWR	Voltage standing wave ratio
MPA	Microstrip patch antenna
SMA	Subminiature version A connector
VNA	Vector Network Analyzer
CPW	Coplanar Waveguide
ACS	Asymmetrical Coplanar Strip
BW	Impedance Bandwidth

TABLE OF CONTENTS

DEDICATIONS I

ACKNOWLEDGEMENTS II

ABSTRACT III

LIST OF SYMBOLS IV

LIST OF ABBREVIATION VI

TABLE OF CONTENTS VII

LIST OF FIGURES X

LIST OF TABLES XII

INTROUCTION…. 1

Chapter 1: Introduction to microstrip patch antenna

1.1 Introduction 2

1.2 Objective 2

1.3 Microstrip Antenna 2

1.3.1 Advantages and Disadvantages 4

1.4 Feeding Methods 4

1.5 Rectangular Patch 6

1.5.1 Transmission line model 6

1.5.2 The cavity models 6

1.6 Fringing Effects 7

1.7 Effective Length, Effective Width and Resonant Frequency 8

1.8 Antenna Parameters 9

1.8.1 Impedance bandwidth 9

1.8.2 Gain 10

1.8.3 Radiation pattern 10

1.8.4 Efficiency 11
1.8.5 Impedance matching 11
1.8.6 Effect of ground 12
1.8.7 Voltage standing wave ratio 12
1.8.8 Return loss 13
1.9 Conclusion 13

Chapter 2: Octagonal ring antenna

2.1 Introduction 14
2.2 Octagonal Monopole Antenna 14
2.3.1 Antenna structure and design procedure 14
2.3.2 Simulation results 15
2.3.3 Current distribution 18
2.3 Octagonal ring antenna 19
2.3.1 Single ring monopole antenna 19
2.3.2 Simulation results 19
2.3.3 The effect of changing the width $\boldsymbol{t}$ 20
2.3.1 The effect of changing the radius $\boldsymbol{Ro}$ 20
2.4 Concentric Octagonal Ring based Antenna 21
2.5 Radiation pattern 25
2.6 Conclusion 27

Chapter 3: Triple band antenna

3.1 Introduction 27
3.2 Antenna design and configuration 27
3.3 Simulation Results 29

3.4 Current distribution..... 31
3.5 Radiation pattern..... 33
3.6 Fabrication and Measurement..... 34
3.7 Size reduction 37
3.7.1 Patch size reduction 37
3.7.2 Antenna size reduction 37
3.8 Conclusion 38
GENERAL CONCLUSION ……. ……..……..……..39
REFERENCES……..……...…40
.

LIST OF FIGURES

Chapter 1: Introduction to microstrip patch antenna

Figure 1. 1 : Microstrip patch antenna [1]. 3
Figure 1. 2 : Representative shapes of Microstrip patch. 4
Figure 1. 3 : Feeding structures used in microstrip antenna [1] 5
Figure 1. 4 : Rectangular Microstrip patch and its equivalent circuit transmission model [2]. 7
Figure 1. 5 : Field lines radiating from a Patch Antenna. 8
Figure 1. 6: Physical length of rectangular patch. 9

Chapter 2: Octagonal ring antenna

Figure 2. 1:Geometry of octagonal antenna. (a) front view (b) back view (c) side view. 15
Figure 2. 2 :Geometry of different antennas involved in the design development. with $R0 = 7.6mm$, $Lg1 = 8.0mm$. 16
Figure 2. 3 :Simulated return loss S (11) for different patch antenna shapes. 17
Figure 2. 4 :Simulation return loss for different values of Wf1 17
Figure 2. 5:Simulated surface current plot at 2.92 GHz. 18
Figure 2. 6:3D radiation pattern of the octagonal ring antenna at f=2.93GHz. 18
Figure 2. 7: Geometry of the octagonal ring antenna. 19
Figure 2. 8:Geometry of the octagonal ring antenna for Ro=7.6mm 20
Figure 2. 9 Simulated return losses for various t. 21
Figure 2. 10: Simulated return loss for various Ro. 21
Figure 2. 11: Double ring patch antenna. With $g = 4.8$ mm. 22
Figure 2. 12:Return loss of dual octagonal ring antenna. 22
Figure 2. 13: Octagonal ring interconnected by (a) one strip line, (b) two strip lines and (c) four strip lines. 23
Figure 2. 14: Return losses versus frequency for different number of connection strips. 23
Figure 2. 15 :Different position of the connection strip line. 24
Figure 2. 16: Simulated losses for different position of the strip connection. 24
Figure 2. 17: Simulated surface current distribution at different resonant frequencies. 25
Figure 2. 18: 3D radiation patterns of the dual rings' antenna at different frequencies. 26

Chapter 3: Triple band antenna

Figure 3. 1: The geometry of the final structure antenna. (a) front side (b) back side. 28
Figure 3. 2:Evaluation stages of antenna. 28
figure 3. 3:Simulated return losses versus frequency of proposed antenna for the different designs..29
Figure 3. 4:Simulated return losses of the proposed antenna for various g. 30
Figure 3. 5:Return loss of the proposed antenna, R1 is varying while t and g are kept constants.....31
Figure 3. 6:The return loss of the proposed antenna, t is varying while R1 and g are kept constants. 31
Figure 3. 7:Average current distributions of the proposed antenna at 2.34, 3.5 and 5.5 GHz.....32
Figure 3. 8: 3D radiation patterns of the proposed antenna at different frequencies.....33
Figure 3. 9 :Radiation patterns of the proposed antenna different frequencies. 34
Figure 3. 10:Photograph of the fabricated tri-band antenna prototype. (a) front view (b) back view. 35
Figure 3. 11:The measured S11 displayed in the VNA screen. 35
Figure 3. 12:Simulated and measured return losses of the proposed antenna. 36
Figure 3. 13: Comparison between the proposed patch and the octagonal patch 37
Figure 3. 14:: Comparison between the proposed structure and the conventionnel octagonal patch antenna footprints.....37

LIST OF TABLES

Table.3. 1:The dimension of the proposed antenna. 27
Table.3. 2 :Comparison between proposed antenna size along with applications bands with others..36

Chapter 1

Introduction to microstrip patch antenna

1.1 Introduction

An antenna can be explained as a transitional structure between free space and a guiding device. Consider a basic mobile phone or a TV or even a radio; all of these devices contain a simple, low profile, light weight, low-cost device for transmission and reception of signals called a microstrip antenna. Microstrip antennas have developed considerably during the past few decades, which have helped in overcoming many of its limitations. There has been a series of developments in the feeding techniques size, thickness, materials, and design. These developments have helped us in increasing the bandwidth and the gain of the antennas. Reducing in the size of the antenna makes it portable and more convenient to use. Microstrip antennas being easy to design and manufacture are used in various fields where low-profile antennas are required.

1.2 Objective

The project is aimed at designing a Microstrip Antenna (MSA) which can work on at three commercially useful bands in range (from 2 GHz to 7 GHz) with acceptable input impedance and bandwidth characteristics. In order to reach these objectives, the effect of antenna dimensions will be studied and the obtained results will be compared till having an optimal design.

1.3 Microstrip Antenna

Microstrip antenna, as shown in Figure 1.1, consists of a very thin metallic strip (patch) placed a small fraction of a wavelength above a ground plane. The microstrip patch is designed so its pattern maximum is normal to the patch. This is accomplished by properly choosing the mode of excitation beneath the patch. For rectangular patch, the length L of the element is usually $\lambda_0/3 < L < \lambda_0/2$. The strip (patch) and the ground plane are separated by a dielectric sheet (substrate) as shown in Figure 1.1. where λ_0 is wave length in te space.

There are numerous substrates that can be used for the design of microstrip antennas, and their dielectric constants are usually in the range of $2.2 \leq \epsilon_r \leq 12$. The ones that are most desirable

for antenna performance are thick substrates whose dielectric constant is in the lower end of the range because they provide better efficiency, larger bandwidth, loosely bound fields for radiation into space, but at the expense of larger element size.

Thin substrates with higher dielectric constants are desirable for microwave circuitry because they require tightly bound fields to minimize undesired radiation and coupling, and lead to smaller element sizes; however, because their greater losses, they are less efficient and have relatively smaller bandwidths. Since microstrip antennas are often integrated with other microwave circuitry, a compromise has to be reached between good antenna performance and circuitdesign.

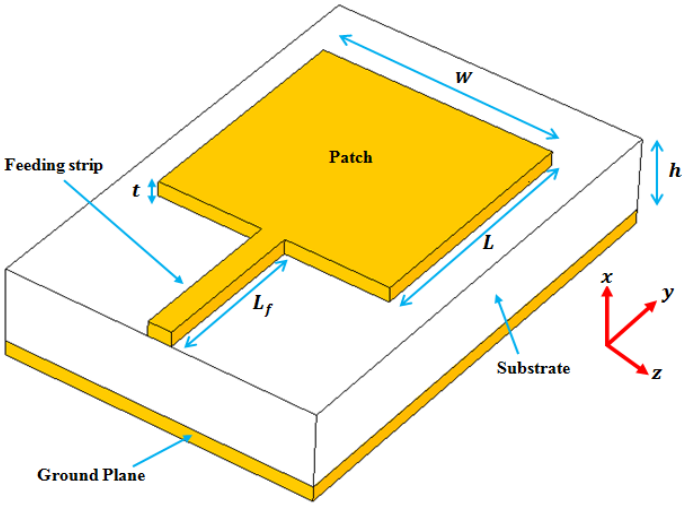

Figure 1. 1 : Microstrip patch antenna [1].

Often microstrip antennas are also referred to as patch antennas. The radiating elements and the feed lines are usually photo etched on the dielectric substrate. The radiating patch may be square, rectangular, thin strip (dipole), circular, elliptical, triangular or any other configuration. These and others are illustrated in Figure 1.2. Square, rectangular, dipole(strip), and circular are the most common because of ease of analysis and fabrication, and their attractive radiation characteristics, especially low cross-polarization radiation. Microstrip dipoles are attractive because they inherently possess a large bandwidth and occupy less space, which makes them attractive for arrays. Linear and circular polarizations can be achieved with either single elements or arrays of microstrip antennas [2].

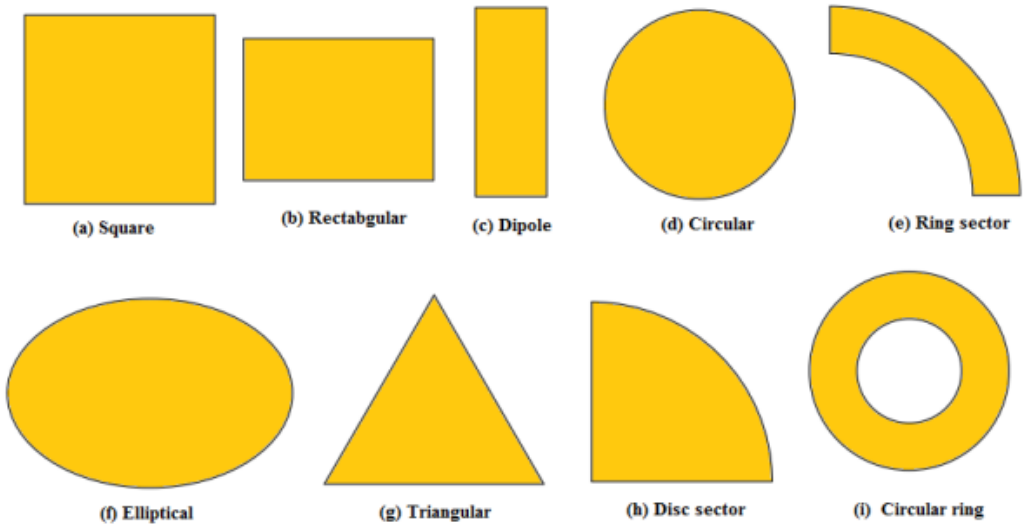

Figure 1. 2 : Representative shapes of Microstrip patch.

1.3.1 Advantages and Disadvantages

Some of their principal advantages are given below:

- Light weight and low fabrication cost.
- Supports both, linear as well as circular polarization.
- Can be easily integrated with microwave integrated circuits.
- Capable of dual and triple frequency operations.
- Mechanically robust when mounted on rigid surfaces.

Microstrip patch antennas suffer from more drawbacks as compared to conventional antennas. Some of their major disadvantages are given below:

- Narrow band width.
- Low efficiency and Gain.
- Extraneous radiation from feeds and junctions.
- Low power handling capacity.
- Surface wave excitation[2][3].

1.4 Feeding Methods

There are many configurations that can be used to feed microstrip antennas. The most popular are the microstrip line, coaxial probe, aperture coupling and proximity coupling. These are displayed in Figure1.3. The microstrip line feed is easy to fabricate, simple to match by controlling the inset position and rather simple to model. However, as the substrate thickness

increases surface waves and spurious feed radiation increases, which for practical designs limit the bandwidth (typically 2-5%). Coaxial-line feeds, where the inner conductor of the coax is attached to the radiation patch while the outer conductor is connected to the ground plane, are also widely used. The coaxial probe feed is also easy to fabricate and match, and it has low spurious radiation. However, it also has narrow bandwidth and it is more difficult to model, especially for thick substrates ($h > 0.02\lambda_0$).

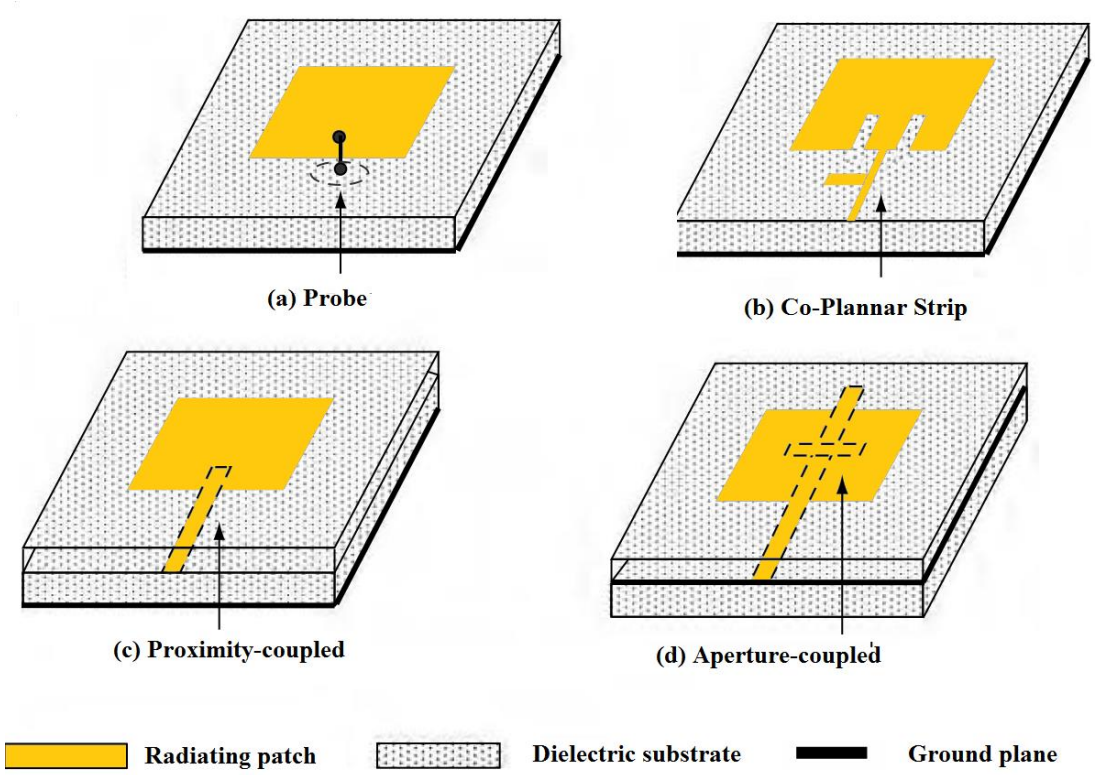

Figure 1. 3 : Feeding structures used in microstrip antenna [1]

Both the microstrip feed line and the probe possesses inherent asymmetries which generate higher order modes which produce cross-polarized radiation. To overcome some of these problems, non-contacting aperture coupling feeds, as shown in Figure1.3 have been introduced. The aperture coupling of Figures1.3 are the most difficult of all four to fabricate and it also has narrow bandwidth.

However, it is somewhat easier to model and has moderate spurious radiation. The aperture coupling consists of two substrates separated by a ground plane. On the bottom side of the lower substrate there is a microstrip feed line whose energy is coupled to the patch through a slot on the ground plane separating the two substrates. This arrangement allows independent optimization of the feed mechanism and radiating element. Typically, a high dielectric material is used for the bottom substrate, and thick low dielectric constant material for the top substrate.

The ground plane between the substrates also isolates the feed from the radiating element and minimizes interference of spurious radiation for pattern formation and polarization purity [3].

1.5 Rectangular Patch

The rectangular patch is by far the most widely used configuration. It is very easy to analyses using both the transmission-line and cavity models, which are most accurate for thin substrates.

1.5.1 Transmission line model

Transmission line model is the easiest method as compared to the rest of the methods. This method represents the rectangular microstrip antenna as an array of two radiating slots, separated by a low impedance transmission line of certain length., it is giving a good physical insight, but is less accurate and it is more difficult to the model coupling [3].

1.5.2 The cavity models

The cavity model provides a formalism describing the fields in the antenna and the radiated fields. Contrary to the transmission line model which is limited to a rectangular patch, there is no *a priori* hypothesis regarding the shape of the radiating element. However, a didactic presentation is facilitated by the existence of analytical mode expressions, which can, for example, apply to either rectangular or circular patches. Here we will only examine the rectangular scenario and the reader should refer to existing literature for other geometries, the equivalent of rectangular micro strip patch antenna is represented as parallel combination of conductance G and reactance B as shown in Figure 1.4, the values G and B are given below which are based on transmission line model expansion [2].

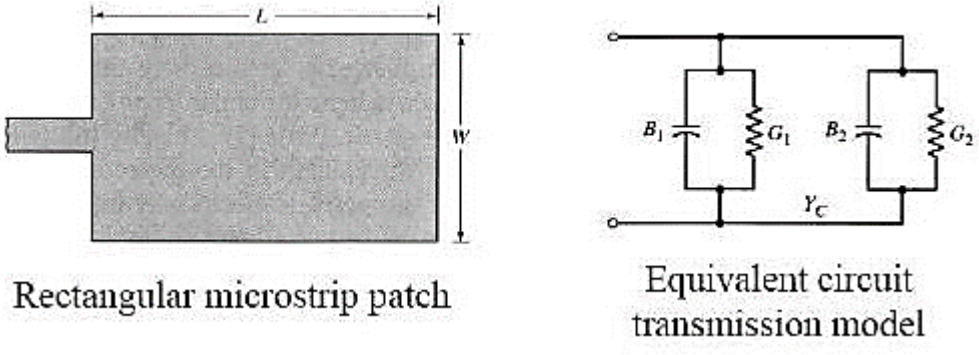

Figure 1. 4 : Rectangular Microstrip patch and its equivalent circuit transmission model [2].

1.6 Fringing Effects

Because the dimensions of the patch are finite along the length and width, the fields at the edges of the patch undergo fringing. This is illustrated along the length in Figure: 1.5. The same applies along the width. The amount of fringing is a function of the dimensions of the patch and the height of the substrate.

For the principal E-plane (xy -plane) fringing is a function of the ratio of the length of the patch $L$to the height $h$of the substrate L/h and the dielectric constant ϵ_r of the substrate. Since for microstrip antennas $L/h >> 1$, this is a nonhomogeneous line of two dielectrics typically the substrate and air. The most of the electric field lines reside in the substrate and parts of some lines exist in air. As$L/h >> 1$and$\epsilon_r >> 1$, the electric field lines concentrate mostly in the substrate. Fringing in this case makes the microstrip line look wider electrically compared to its physical dimensions. Since some of the waves travel in substrate and some in air, an effective dielectric constant $\epsilon_{r_{eff}}$is introduced to account for fringing and the wave propagation in the line. For lower frequencies the effective dielectric constant is given by [1]:

$$\text{For} \quad \frac{W}{h} > 1$$

$$\epsilon_{reff} = \frac{\epsilon_r + 1}{2} + \frac{\epsilon_r - 1}{2}\left[1 + 12\frac{h}{W}\right]^{-1/2} \tag{1.1}$$

To introduce the effective dielectric constant, let us assume that the center conductor of the microstrip line with its original dimensions and height above the ground plane is embedded into one dielectric, as shown in Figure 1.5. The effective dielectric constant is defined as the dielectric constant of the uniform dielectric material so that the line of Figure1.5 has identical electrical characteristics, particularly propagation constant, as the actual line of Figure 1.5.For a line with air above the substrate, the effective dielectric constant has values in the range of $1 < \epsilon_{r_{eff}} < \epsilon_r$. For most applications where the dielectric constant of the substrate is much greater than unity $\epsilon_r >> 1$, the value of $\epsilon_{r_{eff}}$will be closer to the value of the actual dielectric constant ϵ_r of the substrate. The effective dielectric constant is also a function of frequency. As the frequency of operation increases, most of the electric field lines concentrate in the substrate. Therefore, the microstrip line behaves more like a homogeneous line of one dielectric (only the substrate), and the effective dielectric constant approaches the value of the dielectric constant of the substrate.

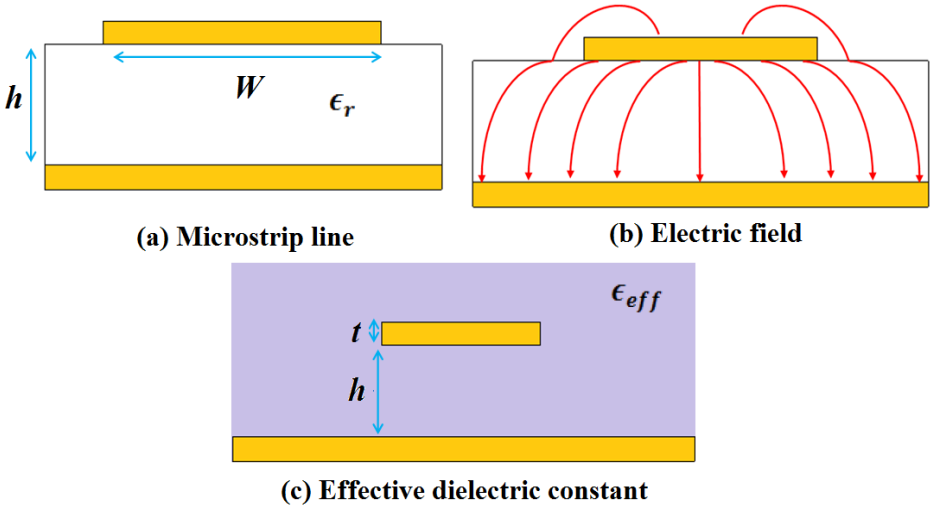

Figure 1. 5 : Field lines radiating from a Patch Antenna.

1.7 Effective Length, Effective Width and Resonant Frequency

Because of the fringing effects, electrically the patch of the Microstrip antenna looks greater than its physical dimensions. For the principal E-plane (xy-plane), this is demonstrated in Figure 1.6 where the dimensions of the patch along its length have been extended on each end by a distance ΔL, which is a function of the effective dielectric constant $\epsilon_{r_{eff}}$and the width- to-height ratio (W/h) [2].

Since the length of the patch has been extended by ΔL on each side, the effective length of the patch.

$$L_{eff} = L + 2\Delta L \tag{1.2}$$

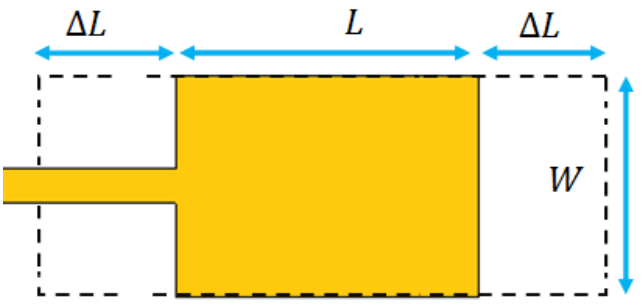

Figure 1. 6: Physical length of rectangular patch.

This microstrip antenna has a rectangular shape with the dimensions of L and W representing length and width of the antenna respectively. There is a conducting surface acting as the ground

plane which is located over a substrate with the thickness h .The resonant frequency $f_{mn}$of the antenna cab be written as

$$f_{mn} = \frac{c}{2\sqrt{\epsilon_{reff}}}\left[\left(\frac{m}{L_{eff}}\right)^2 + \left(\frac{n}{W_{eff}}\right)^2\right]^{1/2} \tag{1.3}$$

where ϵ_{reff} is the effective relative dielectric constant of the dielectric, c is the velocity of electromagnetic waves in free space, m and n integers, and L_{eff} and W_{eff} are the effective dimensions.

1.8 Antenna Parameters

1.8.1 Impedance bandwidth

The frequency range for which the antenna is well matched to its feed is defined as its impedance bandwidth. The impedance bandwidth can be defined in terms of return loss $|S_{11}|$or a voltage standing wave ratio ($VSWR$) over a frequency range. The well-matched impedance bandwidth must totally cover the required operating frequency range for some specified level, such as $VSWR = 2$ or a return loss $|S_{11}|$of less than $10\,dB$. The fractional bandwidth of a microstrip antenna is given by:

$$FBW = \frac{f_h - f_l}{f_c} \tag{1.4}$$

where$f_h$and $f_l$are the upper and the lower cut off frequency of the frequency range respectively and $f_c$is the central frequency of the band. In addition, the antenna bandwidth is inversely proportional to the antenna quality factor $Q_a$and is given by

$$FBW = \frac{1}{Q_a} \tag{1.5}$$

The FBWcan be also expressed using $VSWR$ as:

$$FBW = \frac{VSWR - 1}{Q_a\sqrt{VSWR}} \tag{1.6}$$

The radiation efficiency of an antenna is defined as the power radiated over the input power. It can also be expressed in terms of the quality factors, which for a microstrip antenna can be written as:

$$\eta_a = \frac{Q_a}{Q_{rad}} \tag{1.7}$$

$Q_{rad}$is the quality factor due to radiation. The total quality factor$Q_a$is given by [10]:

$$\frac{1}{Q_a} = \frac{1}{Q_{rad}} + \frac{1}{Q_c} + \frac{1}{Q_d} + \frac{1}{Q_{sw}} \tag{1.8}$$

where Q_c, $Q_a$and Q_{SW}account for quality factors associated with losses caused byconductivity of the patch, substrate dielectric and surface wave, respectively.

1.8.2 Gain

Gain is a parameter which measures the degree of directivity of the antenna's radiation pattern. A high-gain antenna will preferentially radiate in a particular direction. The antenna gains or power gain of an antenna is defined as the ratio of the intensity (power per unit surface) radiated by the antenna in the direction of its maximum output at an arbitrary distance divided by the intensity radiated at the same distance by a hypothetical isotropic antenna [2]. The gain is given by:

$$G = \eta_a D_0 \tag{1.9}$$

1.8.3 Radiation pattern

The radiation pattern of an antenna is a plot of the relative field strength of the radio waves emitted by the antenna at different angles. It is represented by a three-dimensional graph or polar plots of the horizontal and vertical cross sections. The pattern of an ideal isotropic antenna, which radiates equally in all directions, would look like a sphere. Many non- directional antennas, such as monopoles and dipoles, emit equal power in all horizontal directions, with the power dropping off at higher and lower angles; this is called an omnidirectional pattern and when plotted looks like a torus or donut.

The radiation of many antennas shows a pattern of maxima or "lobes" at various angles separated by "nulls", angles where the radiation falls to zero. This is because the radio waves emitted by different parts of the antenna typically interfere, causing maxima at angles where the radio waves arrive at distant points in phase, and zero radiation at other angles where theradio waves arrive out of phase. In a directional antenna designed to project radio waves in a particular direction, the lobe in that direction is designed larger than the others and is called the "main

lobe". The other lobes usually represent unwanted radiation and are called "side lobes". The axis through the main lobe is called the "principal axis" or "bore sight axis"[2]

1.8.4 Efficiency

Efficiency of a transmitting antenna is the ratio of power actually radiated in all directions to the power absorbed by the antenna terminals. The power supplied to the antenna terminals which is not radiated rather converted into heat. This is through loss resistance in the antenna's conductors but can also be due to dielectric or magnetic core losses in antennas using such components. Such loss effectively robs power from the transmitter requiring a stronger transmitter in order to transmit a signal of a given strength. Note that antenna efficiency is a separate issue from impedance matching, which may also reduce the amount of power radiated using a given transmitter. If an SWRmeter reads 150 W of incident power and 50 W of reflected power that means that 100 W have actually been absorbed by the antenna ignoring transmission line losses. How much of that power has actually been radiated cannot be directly determined through electrical measurements at (or before) the antenna terminals, but would require (for instance) careful measurement of field strength [2].

1.8.5 Impedance matching

Maximum power transfer requires matching the impedance of an antenna system looking into the transmission line to the complex conjugate of the impedance of the receiver or transmitter. In the case of a transmitter, the desired matching impedance might not correspond to the dynamic output impedance of the transmitter as analyzed as a source impedance but rather the design value (typically 50 ohms) required for efficient and safe operation of the transmitting circuitry. The intended impedance is normally resistive but a transmitter may have additional adjustments to cancel a certain amount of reactance in order to "tweak" the match. When a transmission line is used in between the antenna and the transmitter (or receiver), one generally would like an antenna system whose impedance is resistive and near the characteristic impedance of that transmission line in order to minimize the standing wave ratio (SWR) and the increase in transmission line losses it entails, in addition to supplying a good match at the transmitter or receiver itself [3].

1.8.6 Effect of ground

Antennas are typically used in an environment where other objects are present that may have an effect on their performance. Height above ground has a very significant effect on the radiation pattern of some antenna types. When an electromagnetic wave arrives at the surface of an object, two waves are created: one enters the dielectric and the other is reflected. If the object is a conductor, the transmitted wave is negligible and the reflected wave has almost the same amplitude as the incident one. When the object is a dielectric, the fraction reflected depends (among other things) on the angle of incidence. When the angle of incidence is small (that is, the wave arrives almost perpendicularly) most of the energy traverses the surface and very little is reflected. When the angle of incidence is near 90° (grazing incidence) almost all the wave is reflected [4].

1.8.7 Voltage standing wave ratio

Standing wave ratio (SWR)is the ratio of the amplitude of a partial standing wave at an antinode (maximum) to the amplitude at an adjacent node (minimum), in an electrical transmission line.

The SWR is usually defined as a voltage ratio called the $VSWR$, for voltage standing wave ratio. The power standing wave ratio ($PSWR$) is defined as the square of the $VSWR$.

SWR is used as an efficiency measure for transmission lines, electrical cables that conduct radio frequency signals, used for purposes such as connecting radio transmitters and receivers with their antennas, and distributing cable television signals. A problem with transmission lines is that impedance mismatches in the cable tend to reflect the radio waves back toward the source end of the cable, preventing all the power from reaching the destination end. SWR measures the relative size of these reflections. An ideal transmission line would have an $SWR$of 1:1, with all the power reaching the destination and no reflected power. An infinite SWR represents complete reflection, with all the power reflected back down the cable. The SWR of a transmission line can be measured with an instrument called an SWR meter, and checking the $SWR$is a standard part of installing and maintaining transmission lines [2].

The voltage standing wave ratio is then equal to:

$$VSWR = \frac{1 + |\boldsymbol{\Gamma}|}{1 - |\boldsymbol{\Gamma}|} \tag{1.10}$$

Where

$$\mathbf{\Gamma} = \frac{Z_L - Z_0}{Z_L + Z_0} \tag{1.11}$$

Where $\mathbf{\Gamma}$ is reflection coefficient,$Z_L$load impedance and Z_0 ischaracteristic impedance.

1.8.8 Return loss

The return loss is the loss of signal power resulting from the reflection caused at a discontinuity in a transmission line. This discontinuity can be a mismatch with the terminating load or with a device inserted in the line. It is usually expressed as a ratio in decibels(dB):

$$RL(dB) = -10\log_{10}\left(\frac{P_i}{P_r}\right) \tag{1.12}$$

where RL (dB) is the return loss in dB,P_i is the incident power and P_r is the reflected power. Return loss is related to both standing wave ratio (SWR) and reflection coefficient (Γ). Increasing return loss corresponds to lower SWR. Return loss is a measure of how well devices or lines are matched. A match is good if the return loss is high. A high return loss is desirable and results in a lower insertion loss. Return loss is used in modern practice in preference to SWR because it has better resolution for small values of reflected wave. The S-parameter S_{11} from two-port network theory is frequently also called return loss.

1.9 Conclusion

This chapter gives the fundamental parameters of a microstrip antenna. A brief description of a microstrip antenna was provided, then some of its important parameters are presented in details. The aim of the second chapter is to design a microstrip antenna and simulate its main parameters namely return loss, gain and radiation pattern with help of a full wave simulator.

Chapter 2

Octagonal ring antenna

2.1 Introduction

A microstrip patch antenna can be used alone or in combination with other elements as a part of an array. In either case, the designer should have a step-by-step element design procedure. In addition, the shape of patch can take different geometrical forms such as rectangular, circular, triangular, elliptical, square and any other configuration. More complex patterns based on regular shapes have been introduced to meet the requirements of a certain applications [5]. Consequently, the choice of the shape depends on specific limitations such as size, radiation pattern, gain, bandwidth etc. Basically, the operating modes of the antenna depends on the patch dimensions, the substrate characteristics as well as the feeding configuration.

In this chapter, a new approach based on concentric octagonal rings concept for compact and multimode operation will be proposed and studied. Firstly, a basic shaped patch geometry including triangular, square, pentagonal, hexagonal, heptagonal and octagonal will be designed and studied. Secondly, the resulted octagonal structure will be loaded with an octagonal slot such that an octagonal shaped ring patch antenna will be obtained. Finally, a second octagonal ring is loaded to the first ring then a connection strip line is introduced. The six (6) structures, namely triangular patch, square patch, pentagonal patch, hexagonal patch, heptagonal patch and octagonal ring antennas will be studied in the following sections.

2.2 Octagonal Monopole Antenna

2.3.1 Antenna structure and design procedure

Figure 2.1 shows the geometry of the proposed octagonal monopole antenna along with its details. The proposed structure consists of an octagonal shape radiating section fed with trapezoidal shape microstrip line and trapezoidal ground plane. The selected geometry is the result of an evolution study which consider six different shaped monopole having same radius Ro as depicted in Figure 2.2. The tapered feed line and the trapezoidal partial ground plane are used for better impedance matching purpose.

2.3.2 Simulation results

The shapes vary according to the number of sides, including six polygons staring from the triangle, square until reaching the octagonal shape as shown in Figure 2.2. However, all considered shapes have same patch radius R_o and the antenna ground plane and feeding structure dimensions are kept unchanged. The different structures are designed using FR-4 substrate with thickness $hs = 1.6mm$ relative permittivity $\epsilon_r = 4.3$ and loss tangent $\delta = 0.02$ and they are simulated and investigated by means of the full-wave commercial software CST Microwave Studio. The proposed antenna dimensions are given in Table 2. 1.

Table 2. 2 The dimension of the octagonal shape antenna.

Parameter	Value (mm)	Parameter	Value (mm)
Ws	20	**L_f**	10
Ls	25.5	**Wg**	8
W_{f1}	2	**Lg**	5
W_{f2}	3	**Ro**	7.6

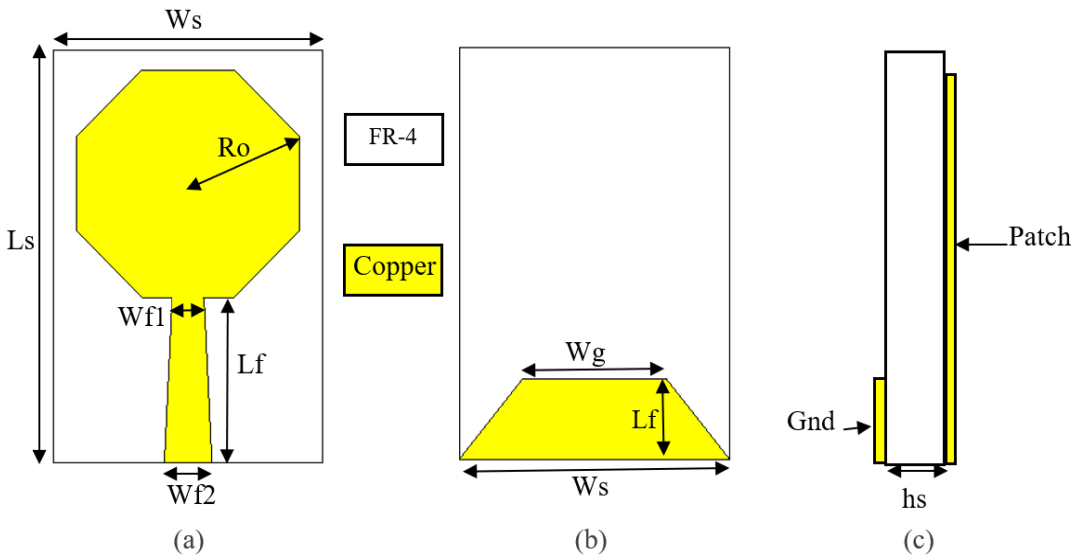

Figure 2. 1:Geometry of octagonal antenna. (a) front view (b) back view (c) side view.

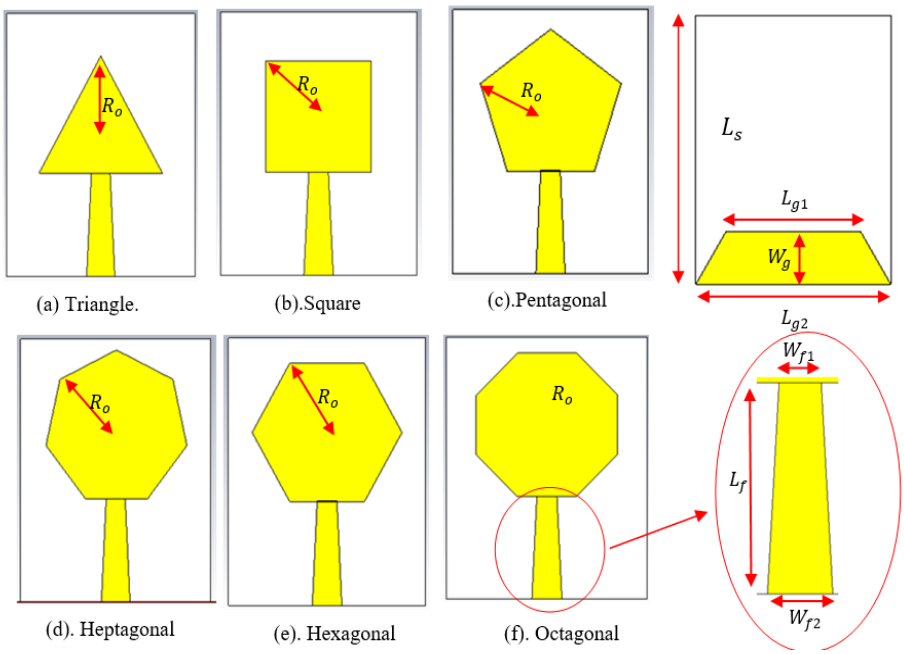

Figure 2. 2 :Geometry of different antennas involved in the design development. with $R_0 = 7.6mm$, $Lg_1 = 8.0mm$.

The simulated reflection coefficients for different configuration are depicted in Figure 2.3. It can be seen that; all antennas operate at one single band in the considered range of frequency (from 2GHz to 7GHz). Moreover, it can be concluded that when the polygon's sides number increases to move from one shape to another, the resonant frequency shifts towards lower frequency side leading to size reduction.

The triangular patch depicted in Figure 2.2 (a) operates at 3.31 GHz with a return loss of -38.9dB while the square shaped design, shown in Figure 2.2 (b), resonates at 2.9 GHz with return loss level of -32dB. The two bands are not suitable for the 2.4 allotted to WLAN band and more sides in the polygon shaped patch are needed to shift the resonance toward cover the mentioned band. The remaining shapes including pentagonal, hexagonal, heptagonal and octagonal operates at frequency bands close to 2.45 GHz band. It can be seen from the simulated results that the octagonal shaped antenna has the lowest resonant frequency occurring at 2.71 GHz with good return loss level of -30dB. Accordingly, this shape is selected to be used to design compact antenna operating at 2.45 GHz.

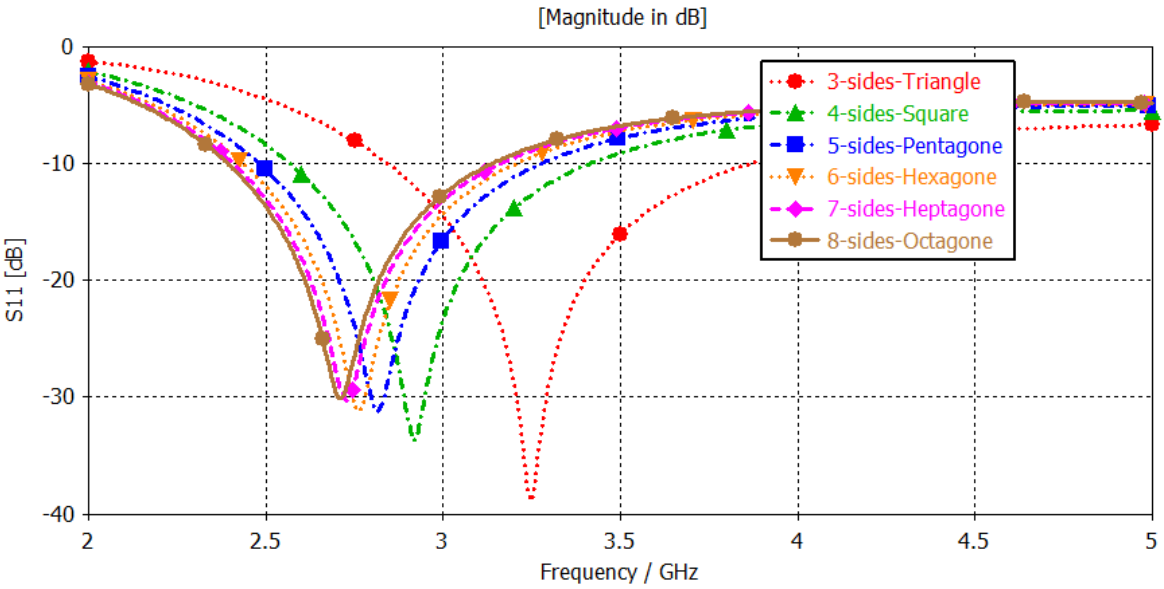

Figure 2. 3 :Simulated return loss S (11) for different patch antenna shapes.

Usually, the first design is not fully optimized and it is necessary to adjust the model to further refine the dimensions. Variation of reflection coefficient for different value of Wf1 is shown in Figure 2.4. It can be seen from the figure that the frequency is shifted towards the left side by increasing the value Wf1 and the three resonant frequencies have a good impedance matching. Furthermore, it is can be clearly noticed from the figure that for Wf1 $= 3mm$, good impedance matching is achieved.

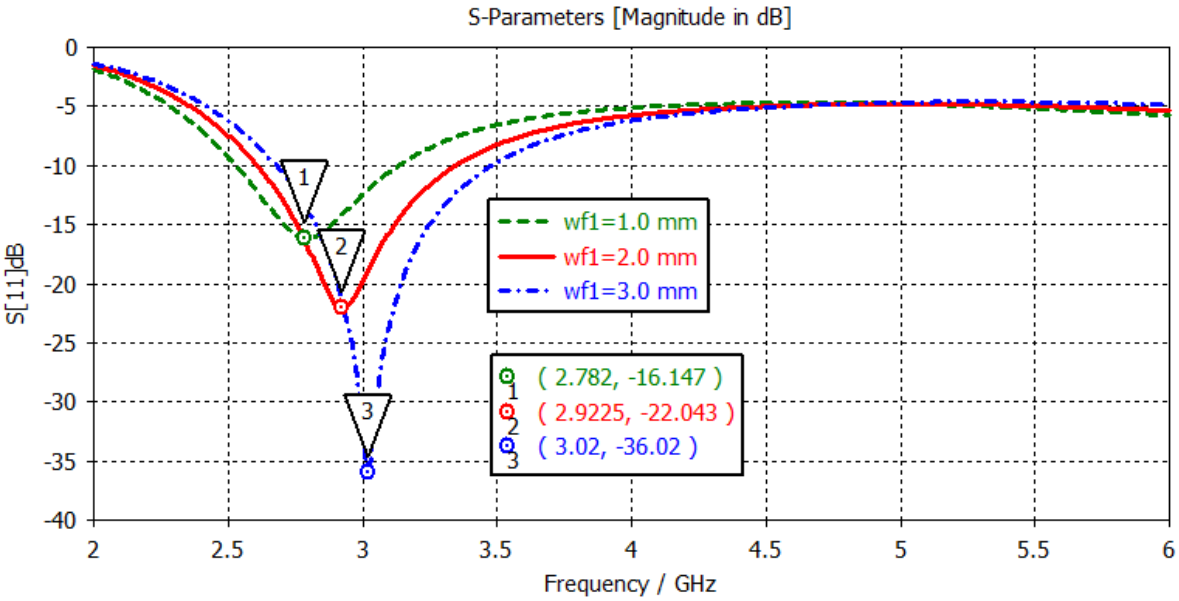

Figure 2. 4 :Simulation return loss for different values of W_{f1}.

2.3.3 Current distribution

The excited surface current distribution for the operating frequency is simulated and it is shown in Figure 2.5. It can be clearly seen that the exited mode is the mode TM11 where the current zeros occur at the upper side of the octagonal patch. Maximum current density is seen at the lowest side of the octagonal patch and on the feedline. Consequently, it can be concluded that this mode is fully controlled by the patch radius Ro.

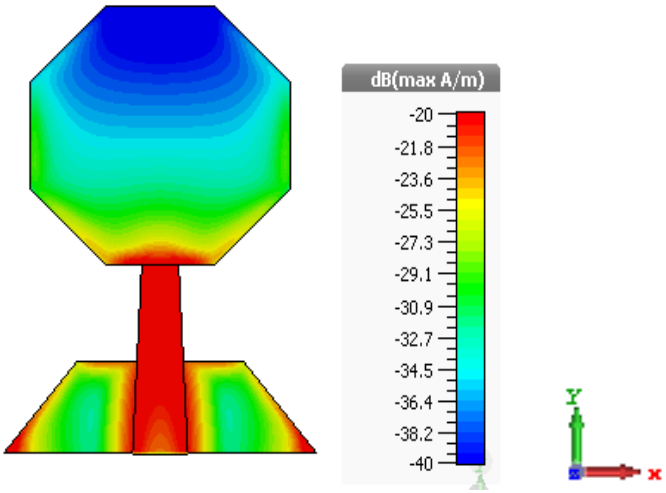

Figure 2. 5:Simulated surface current plot at 2.92 GHz.

The simulated far field of the octagonal monopole antenna is depicted in Figure 3.6. It can be clearly seen from the result; the radiation pattern is omnidirectional in the H-plane (x-z plane) and dipole-like radiation in the E-plane (y-z plane).

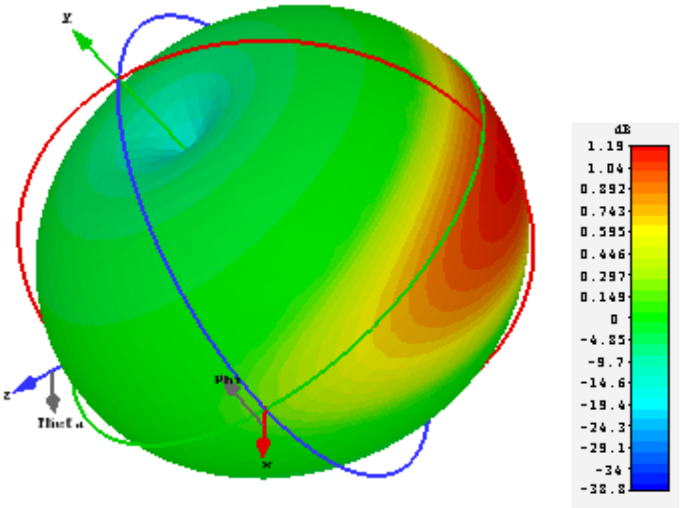

Figure 2. 6:3D radiation pattern of the octagonal ring antenna at f=2.93GHz.

2.3 Octagonal ring antenna

2.3.1 Single ring monopole antenna

To decrease the resonant frequency of the octagonal monopole antenna and cover the 2.4 WLAN band without increasing the antenna patch size and hence downsize the antenna dimension, the octagonal monopole antenna described in the previous section is loaded with an octagonal slot. When the slot is etched from the patch, the resulted antenna is an octagonal ring antenna as depicted in Figure 2.5.

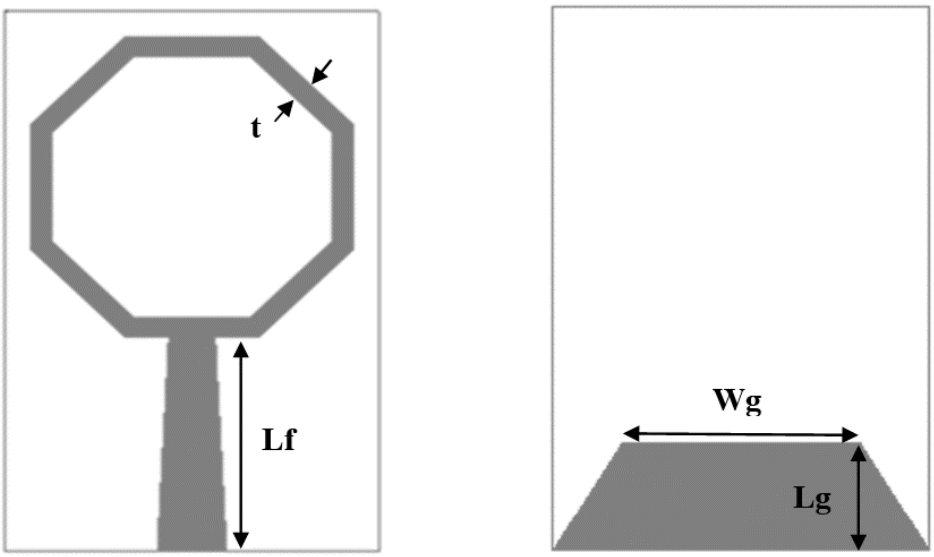

Figure 2. 7: Geometry of the octagonal ring antenna.

2.3.2 Simulation results

The Simulate return losses of the octagonal patch and the derived octagonal ring are presented in Figure 2. 8. It can be seen from the results that the first resonant frequency is shifted from 2.7 GHz to 2.5 GHz by introducing the slot which leads to further size reduction. Furthermore, the octagonal ring antenna operate at two bands.

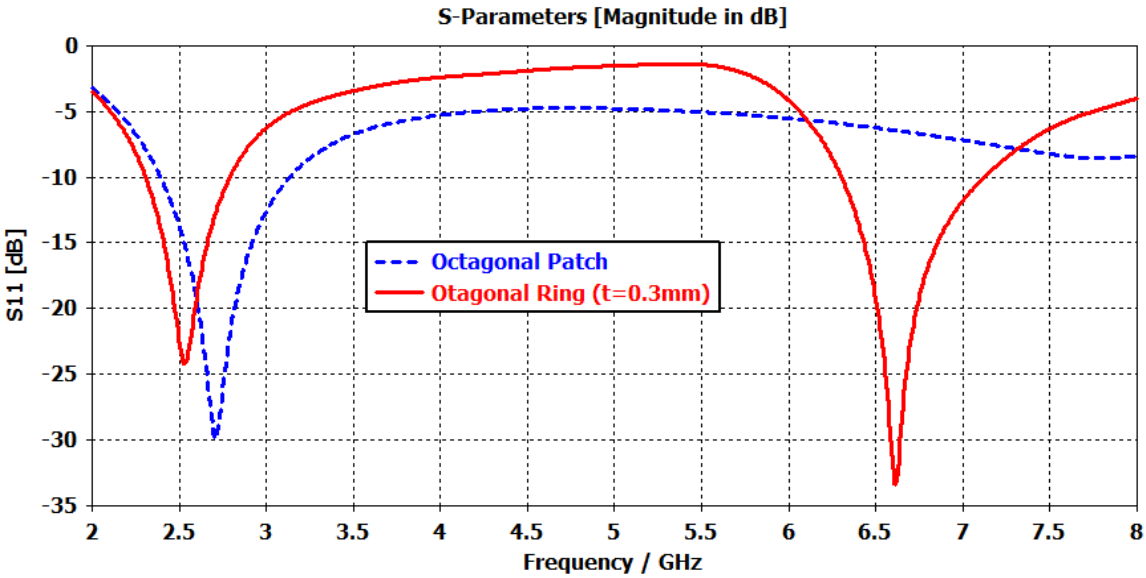

Figure 2. 8:Geometry of the octagonal ring antenna for Ro=7.6mm.

2.3.3 The effect of changing the width t

The effect of varying the parameter t on the return loss is given in Figure 2.9. It can be observed from the figure that the antenna resonates at two frequency bands in the frequency range [2 – 8] GHz. As the width of the octagonal ring t decreases, the first resonant frequency remains unchanged while the second band shifts significantly towards lower frequencies.

2.3.1 The effect of changing the radius Ro

Figure 2.10 illustrates the simulated refection coefficient results when the radius Ro varies from 6.4mm to 8.4mm with a step of 1 mm. It can be observed that as the value of Ro increases, the first resonant frequency shifts towards lower frequencies side while the second resonant frequency decreases significantly. For $Ro = 7.4mm$ the antenna first resonance occurs at 2.45 GHz Accordingly, the antenna operating frequencies can be controlled by mainly changing the value of the key parameter Ro and its first operating band is centered at around 2.45 GHz for $Ro = 7.4mm$.

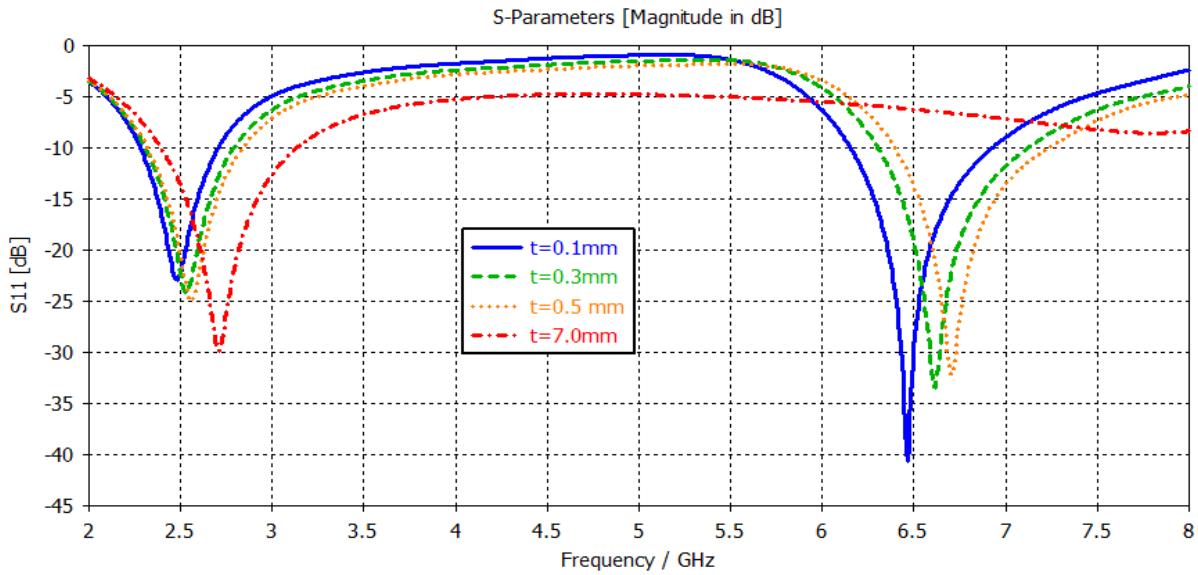

Figure 2. 9 Simulated return losses for various t.

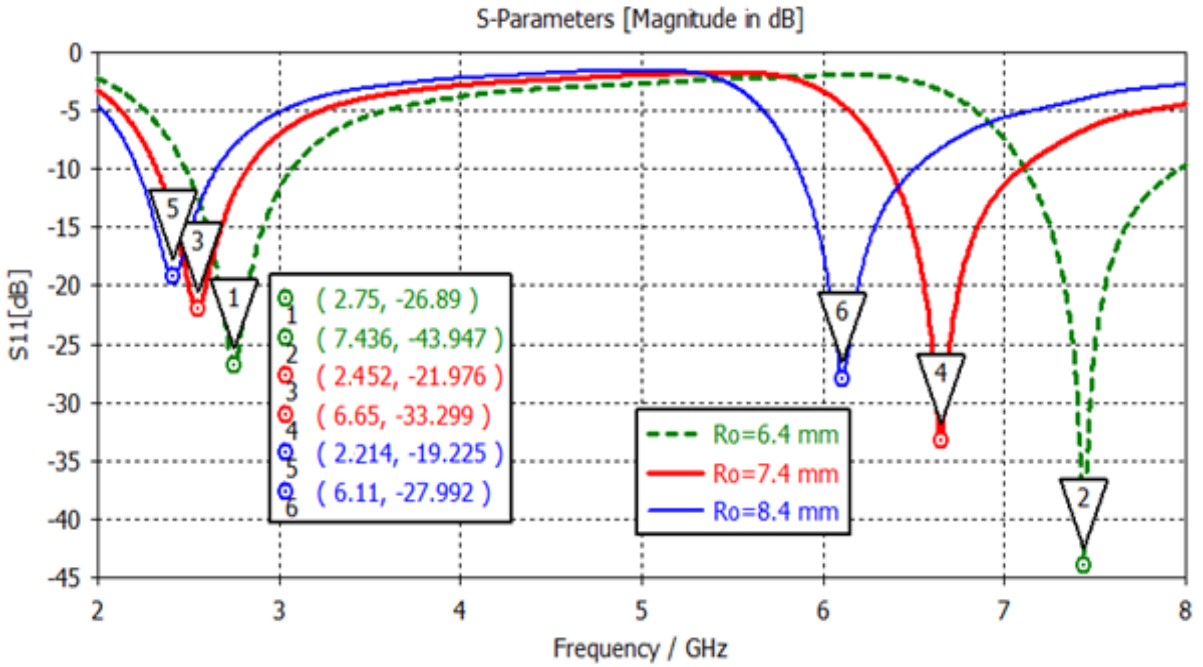

Figure 2. 10: Simulated return loss for various Ro.

2.4 Concentric Octagonal Ring based Antenna

It is clear from the results obtained previously that the investigated antennas operate only in two bands. In order to create a third operating band, additional radiating elements should be introduced to the octagonal ring monopole structure. For this purpose, a second octagonal ring is loaded inside the monopole ring antenna. The two rings are concentric and their geometric configuration is depicted in Figure 2.11.

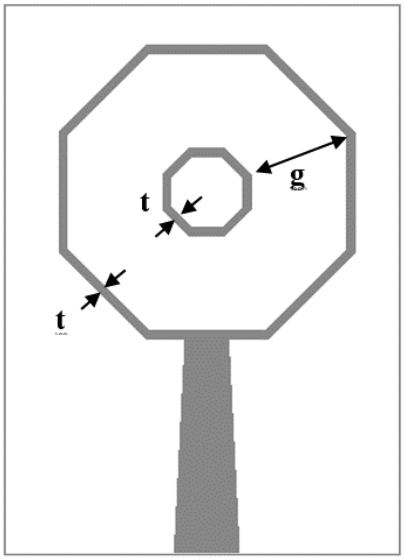

Figure 2. 11: Double ring patch antenna. With $g = 4.8\,mm$.

From the simulated return loss of the antenna presented in Figure 2.12, it is clear that the introduction of the inner ring to the monopole octagonal antenna has no effect on the number of operating modes of the antenna. In order to achieve triple band operation, the two octagonal rings are connected with different number of a one strip lines.

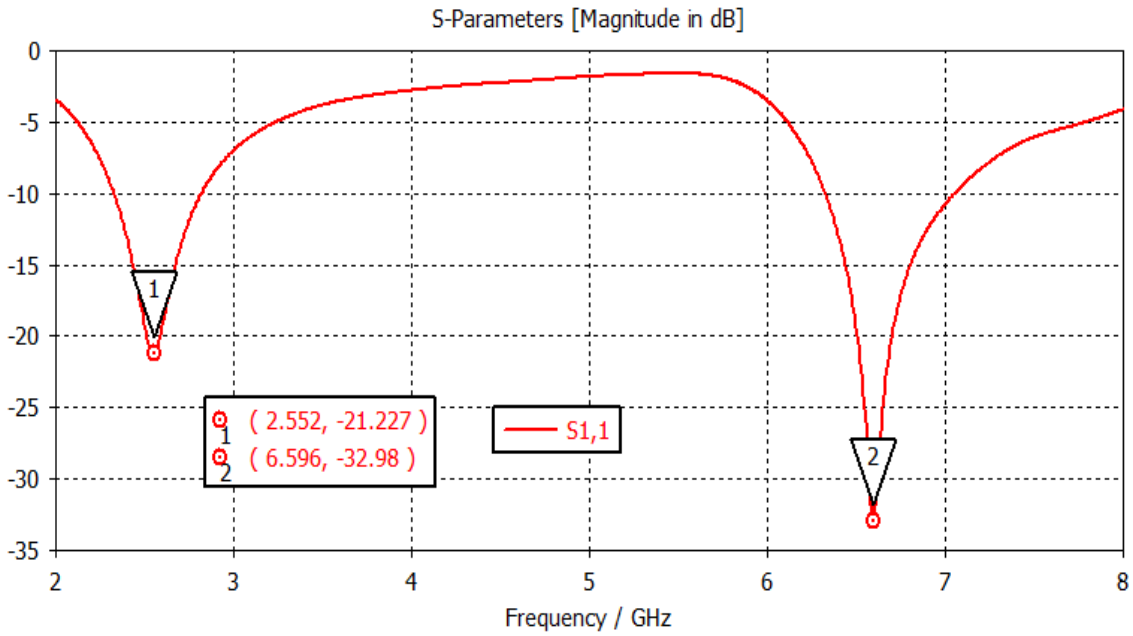

Figure 2. 12:Return loss of dual octagonal ring antenna.

2.4.1 Connection strips number effect

The two rings are connected by one, two and four microstrip lines and their geometrical configurations are shown in Figure 2.13. The connecting strip lines have similar lengths with similar width t as the two radiating rings.

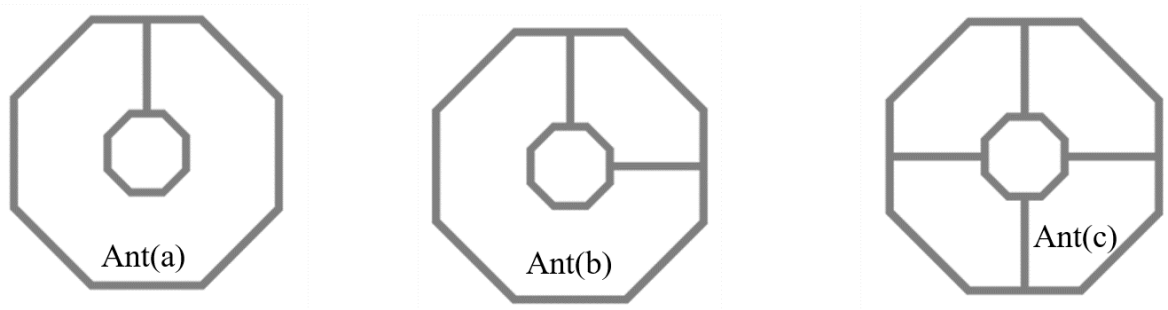

Figure 2. 13: Octagonal ring interconnected by (a) one strip line, (b) two strip lines and (c) four strip lines.

It can be seen, from the simulated return losses presented in Figure 2.14, that Ant (b) with two connection strips and Ant (c) with four connection strips, are dual band antennas while Ant (a) with only one connection strip is a triple band antenna operating at 2.21GHz, 3.62 GHz and 7.12 GHz with return loss level of -14.47dB, -15dB and -31.2dB respectively. Since the main focus of this work is the design of compact triple band antenna, only Ant(a) will be considered in the coming sections.

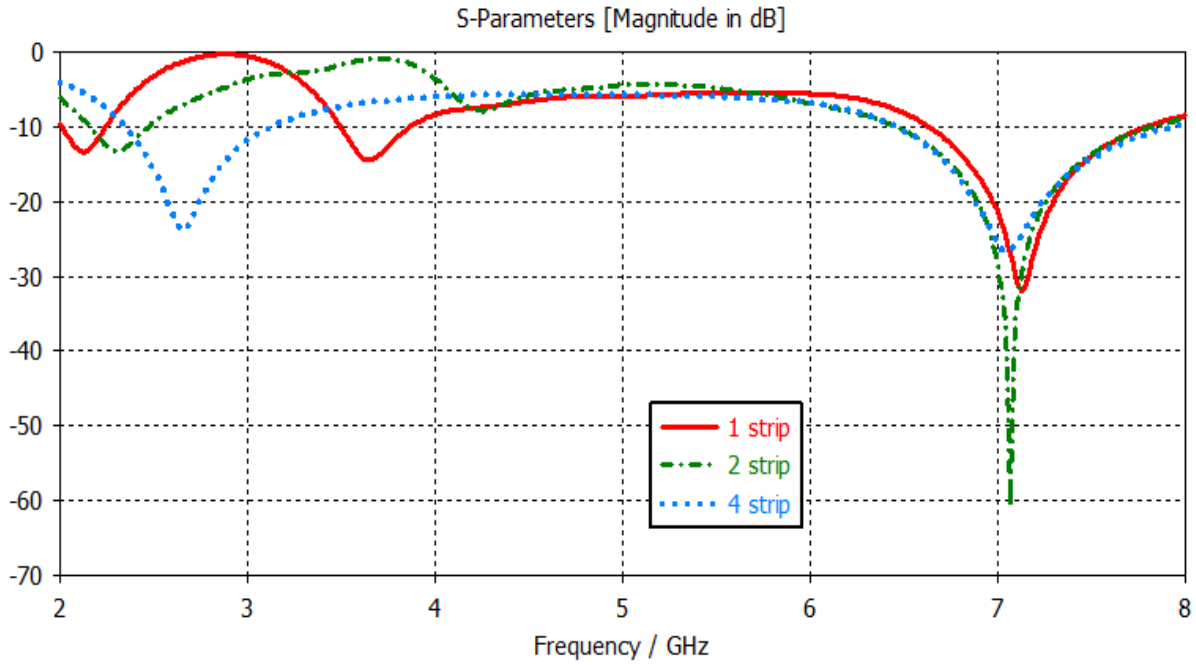

Figure 2. 14: Return losses versus frequency for different number of connection strips.

2.4.2 Position of the connection strip

The simulated return losses of the proposed antenna for different positions of the connecting strip are shown in Figure 2.15. It is clearly seen from that the connection position affects significantly the antenna operating bands and all the investigated position of the strip line connection give rise to triple band operation. However, when the connection is established at position E (proposed antenna), three operating bands are also obtained with better impedance matching for the first and second operating bands. It is worth to mention that the remaining positions of the connection are not considered in the study due to the structure symmetry.

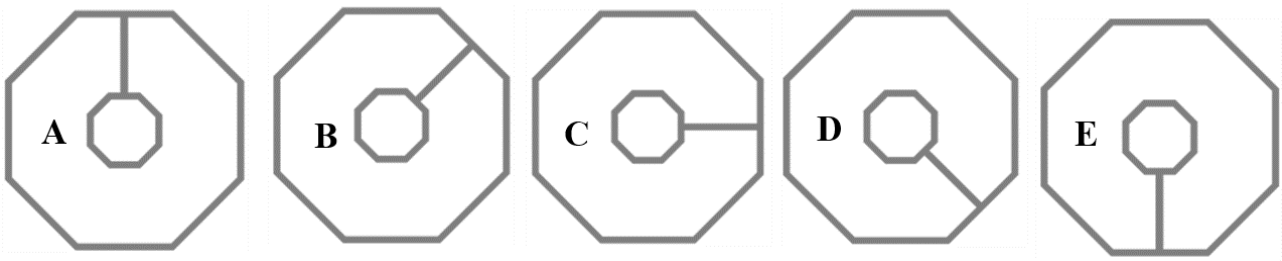

Figure 2. 15 :Different position of the connection strip line.

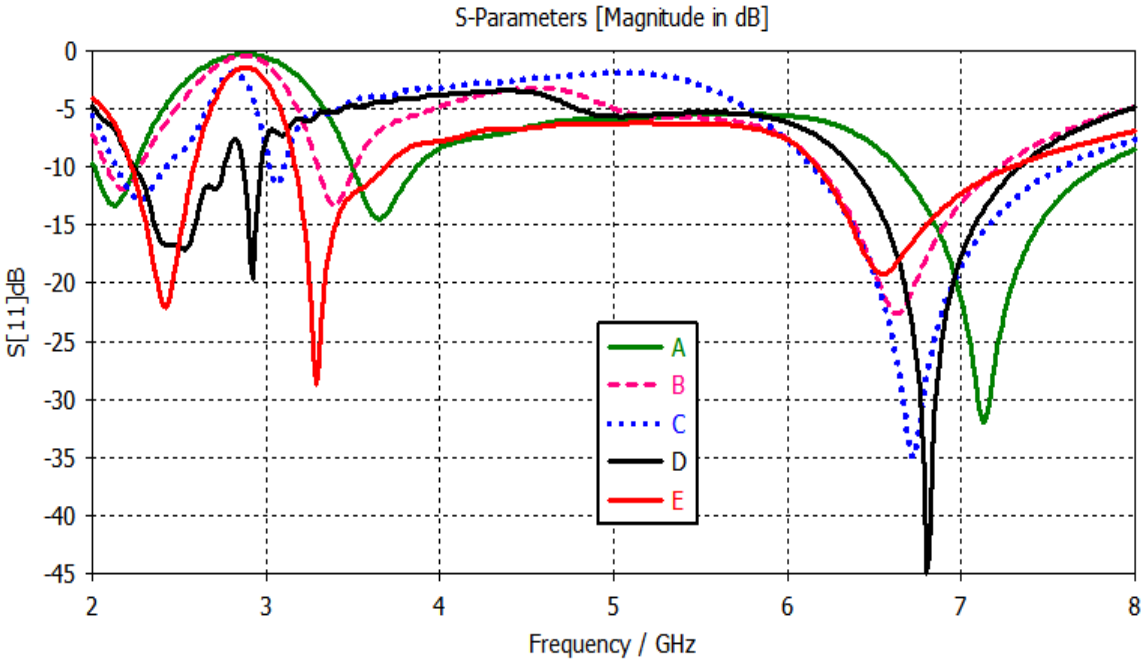

Figure 2. 16: Simulated losses for different position of the strip connection.

After several studies and based on the results obtained, the final shape of the tri-band antenna is reached. The structure consists of two interconnected rings. From Figure 2.16, it is seen that the antenna operates in three bands: 0.36 GHz (2.22-2.58) GHz and 0.52 GHz (3.16-3.68) GHz and 1.09 GHz (6.18-7.27) GHz with a good impedance matching.

To further investigate the operating mechanism of the proposed structure, the current distribution at the three resonant frequencies is simulated and shown in Figure. 2.17. It can be seen that, at the first resonant frequency, the current is mostly concentrated on the feedline and on the outer ring, this confirms the fact that this first band is mainly radiated by the outer ring. Consequently, the first resonant frequency can be controlled by changing the radius of the outer ring Ro. The current at the second resonant frequency is mainly concentrated in the strip connection and on the inner ring, hence this second resonance can be tuned by changing the strip line dimension as well as the inner ring radius. At the third resonance frequency, the current is mostly on the outer ring and the connection strip.

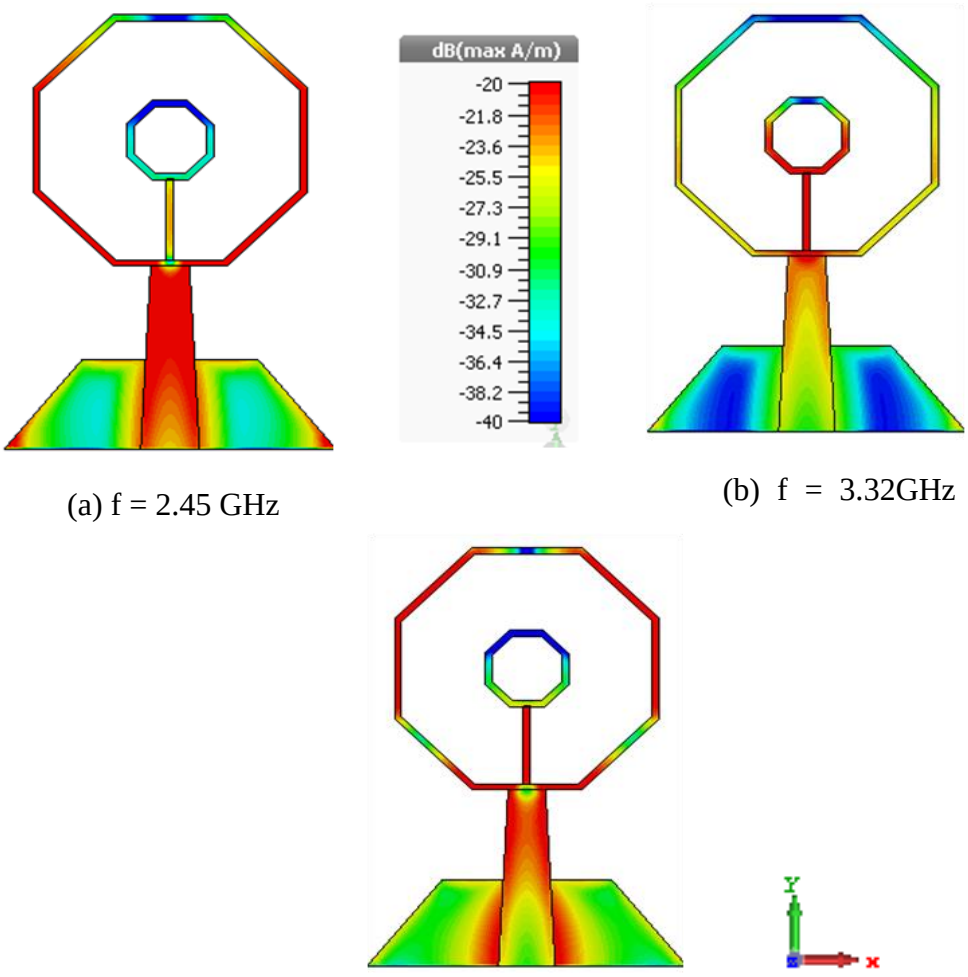

(a) f = 2.45 GHz

(b) f = 3.32GHz

(c) f = 6.53 GHz

Figure 2. 17: Simulated surface current distribution at different resonant frequencies.

2.5 Radiation pattern

The simulated radiation patterns of the proposed antenna at the resonant frequencies are represented in Figure 2.18. It can be seen that, at the first resonance frequency, the antenna exhibits an omnidirectional

radiation pattern in the H-Plane and dipole-like radiation in E-Plane. At the second resonance, similar radiation pattern as the first resonant frequency is observed. Omnidirectional radiation pattern in the H-Plane is observed at the third operating band while the slight distortion in the pattern is occurred in the E-Plane.

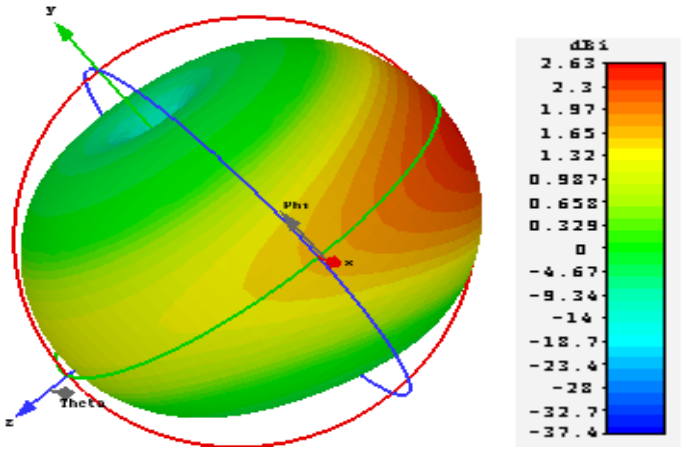

f=2.45 GHz .

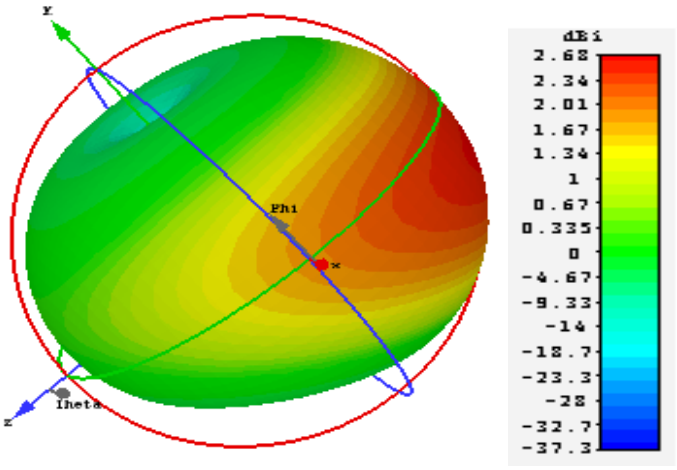

f=3.32GHz.

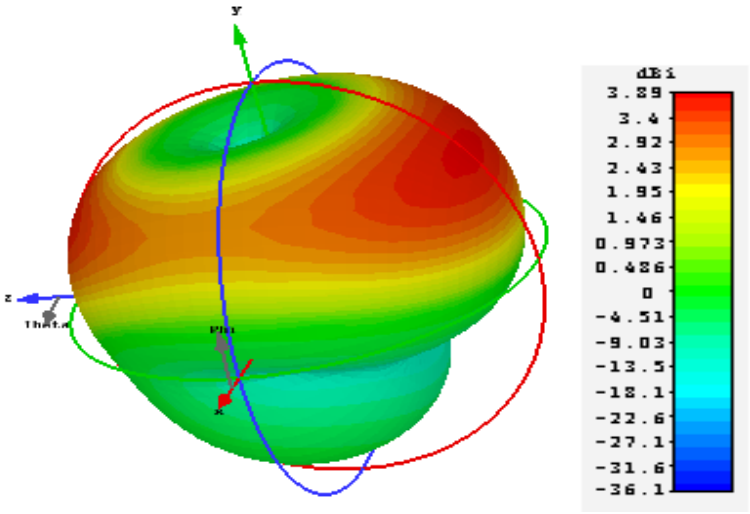

f=6.53 GHz.

Figure 2. 18: 3D radiation patterns of the dual rings' antenna at different frequencies.

2.6 Conclusion

In this chapter, a triple band monopole antenna was designed. The proposed structure operates at three different bands. The first and the second band are useful and cover the 2.4 WLAN band and the 3.5 WiMAX band. However, the last operating band is not suitable for the intended applications. In the next chapter, the designed dual ring triple band antenna will be the basic structure to design a compact antenna which covers the 2.4GHz, 3.5 GHz and 5.5 GHz bands.

Chapter 3

Triple band antenna

3.1 Introduction

The previous chapter dealt with the design step by step of triple band antenna. The procedure to achieve triple band antenna involve at first the analysis of various structure including, triangular, square, pentagonal, hexagonal, heptagonal and octagonal shaped radiating patches. This part has led to the selection of the octagonal as the basic shape since it gives the lowest resonance hence achieve size reduction. The second part aimed to create more resonances in order to meet the requirements of triple band operation. The resulted structure, interconnected dual-concentric octagonal ring antenna, operates at three bands.

This aim of this chapter is to design, based on interconnected-dual concentric octagonal ring antenna, an antenna which can operate at specific bands covering the 2.4/5.5WLAN and 3.5 WiMAX application.

3.2 Antenna design and configuration

In this section, the design of a triple band octagonal ring antenna will be presented. The proposed antenna consists of two concentric octagonal rings connected by means of a strip line. Then, each side of outer ring is connected to an octagonal small shaped branch in order to tune the third resonant frequency to cover the intended application. The resulted structure is fed by a tapered feed line and printed on the top side of FR-4 substrate with relative permittivity of 4.3, loss tangent of 0.02 and thickness of 1.6mm. The other side of the substrate is a partial ground plane as depicted in Figure 3.1. The proposed antenna dimensions are given in table 3.1.

Table.3. 1:The dimension of the proposed antenna.

Parameter	Value (mm)	Parameter	Value (mm)
W_s	20	**L_f**	10
L_s	25.5	**W_g**	8
W_{f1}	2	**L_g**	5
W_{f2}	3	**R_1**	1.7
g	4.8	**R_O**	7.6
t	0.4	**R_i**	2.4

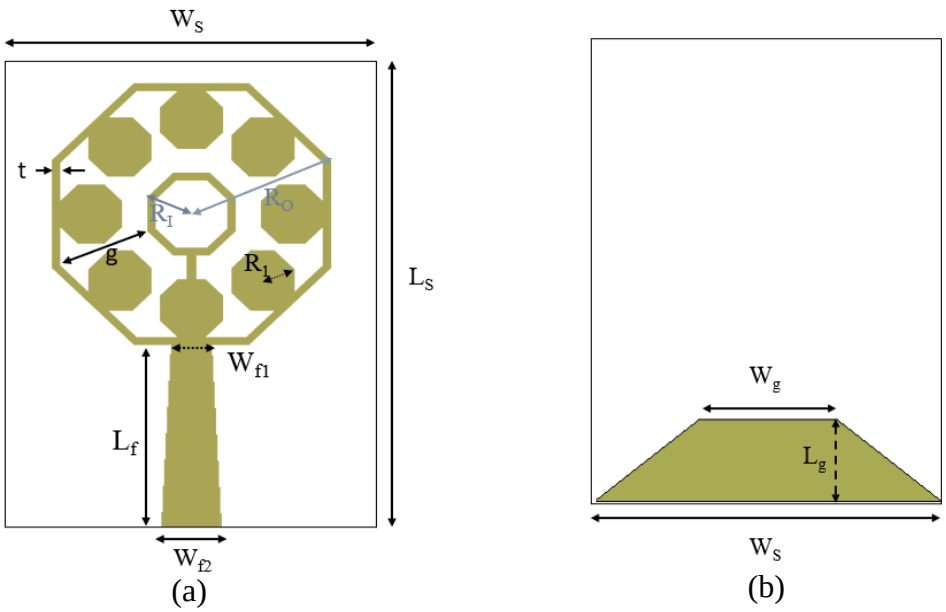

Figure 3. 1: The geometry of the final structure antenna. (a) front side (b) back side.

The evolution stages of the proposed antenna are performed in four different steps. The first, second, and the third designs are presented in detail in the previous chapter. The evolution starts with a simple octagonal shaped monopole antenna Ant.1 as shown in Figure 3.2. Then an octagonal slot is loaded to Ant.1 to obtain an octagonal ring structure namely Ant.2. second octagonal ring is loaded in the center of the outer one and connected with a strip line to obtain Ant.3. the last design which is proposed structure is obtained by attaching the inner contour of the outer ring to eight similar octagonal shaped patches. The resulted antenna has small dimensions and operate at three bands centered at 2.34 GHz ,3.5GHz and 5.55GHz covering the 2.4GHz band allotted to WLAN and 3.5/5.5 GHz allocated to WiMAX application.

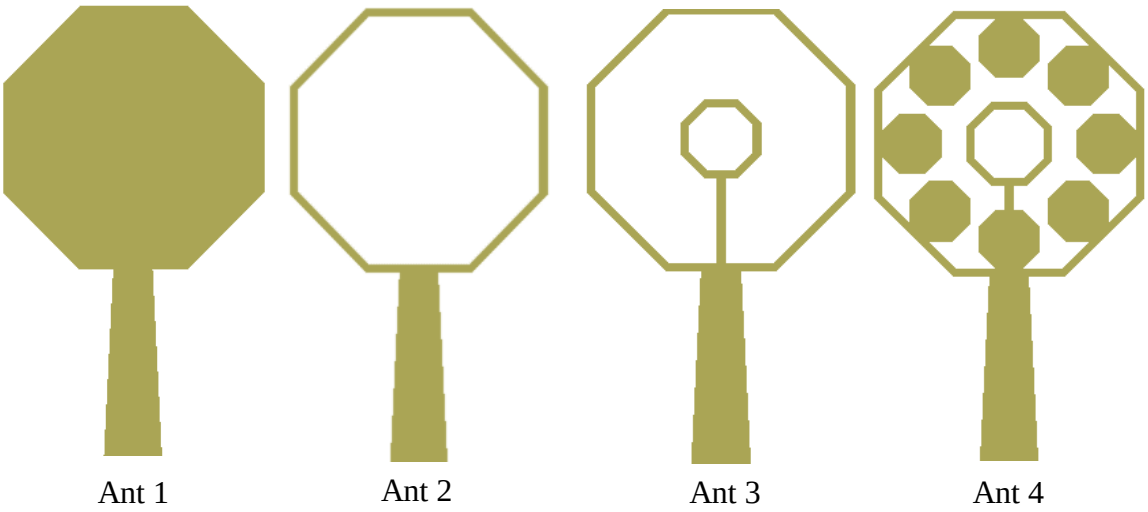

Figure 3. 2:Evaluation stages of antenna.

3.3 Simulation Results

Simulated S_{11} of proposed antennas are represented in Figure 3.3. It is clearly noticed that Ant 1 operates at a single frequency band centered at 2.92 with a return loss level of -22 dB.Ant 2 is a dual band antenna resonating at 2.5 GHz with a return loss of -20 dB and at 6.5 GHz with reflection coefficient of -19 dB.Ant.3 is operating at three bands centered at 2.5 GHz,3.5GHz and 6.8 GHz as can be seen in Figure 3.3. The proposed antenna namely Ant4, is radiating at three bands centered at 2.45 GHz, 3.5 GHz and 5.55 GHz with good impedance matching characteristic with return loss levels of -17 dB, -25dB and -45dB respectively.

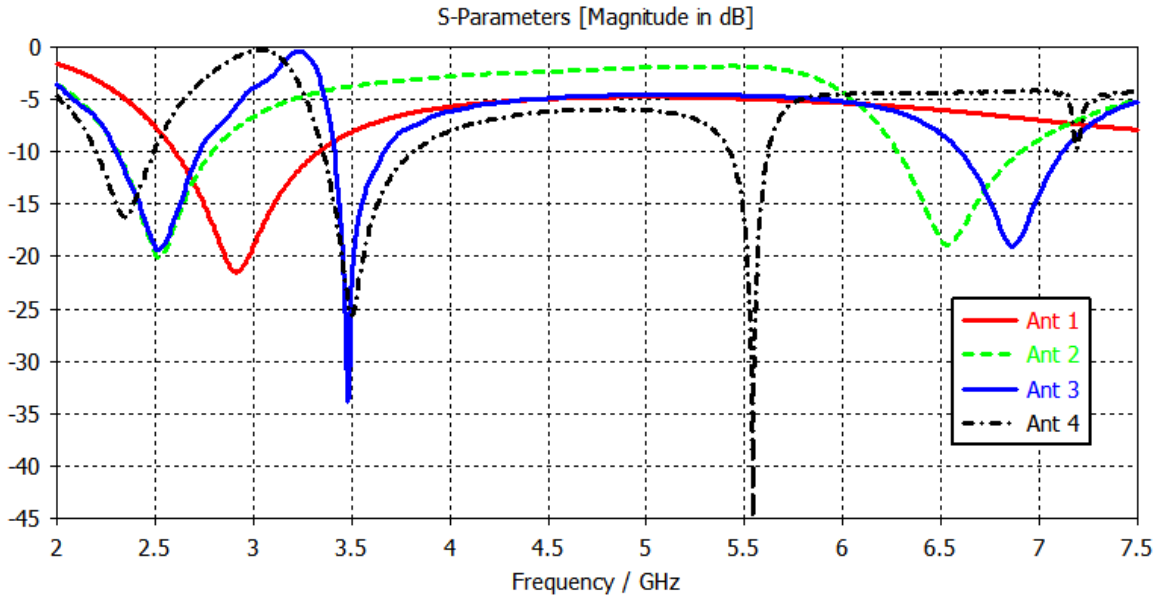

figure 3. 3:Simulated return losses versus frequency of proposed antenna for the different designs.

- **Effect of the gap between two rings (g)**

To further investigate the proposed antenna performance, a parametric study is carried out. Figure 3.4shows the results obtained through simulation of the return-losses characteristics according to the changes in the gap length g while all parameters are kept constants. As the gap increases from 4.6 to 5.0 mm, the second resonant frequency shifts towards higher frequencies. Furthermore, it can be seen that the second band is centered at the desired frequency 3.5 GHz when g = 4.8 mm. Accordingly, the second operating band can be controlled by varying g.

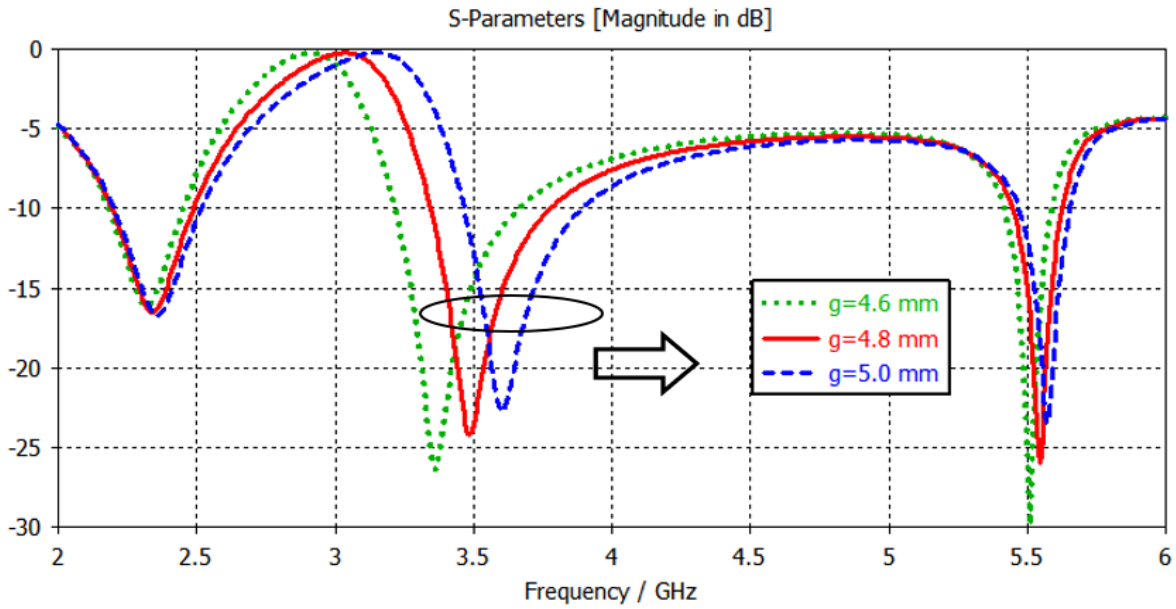

Figure 3. 4:Simulated return losses of the proposed antenna for various g.

- **Effect of the octagonal branches radius (R1)**

The simulated reflection coefficient for different values of the radius R1 is shown in Figure 3.5. It is noticed that by increasing R1 from 1.6 to 1.8 mm, the third resonant frequency shifts towards lower frequency side. The considered value of R1 is 1.7 mm since the corresponding third resonant frequency is centered at 5.55 GHz with good impedance matching. This band tuned by changing the radius R1.

- **Effect of the radiating rings width(t)**

The dependence of the reflection coefficient of the antenna on radiating rings width is shown in Figure 3.5. It can clearly be seen that all resonant frequencies decrease with the increasing of the radiating rings width. In addition, better impedance matching for the third band is achieved by increasing value of t. For t of 0.4mm, the three bands are centered at the desired frequencies of 2.34GHz, 3.5 GHz and 5.5 GHz. Accordingly, antenna size reduction is achieved in term of first resonance.

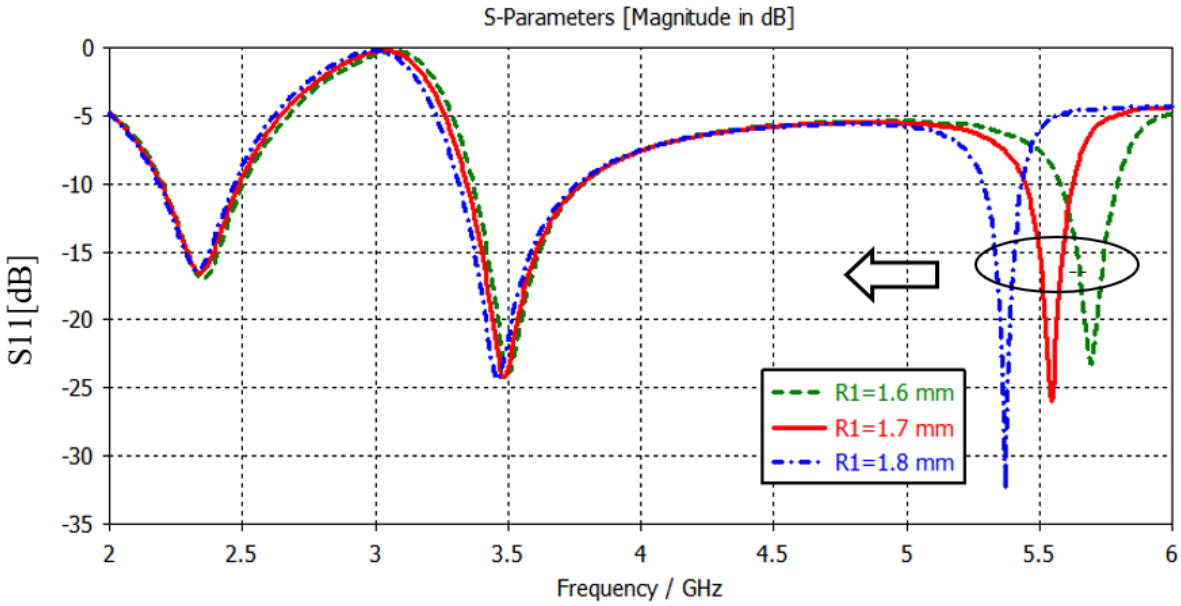

Figure 3. 5:Return loss of the proposed antenna, R1 is varying while t and g are kept constants.

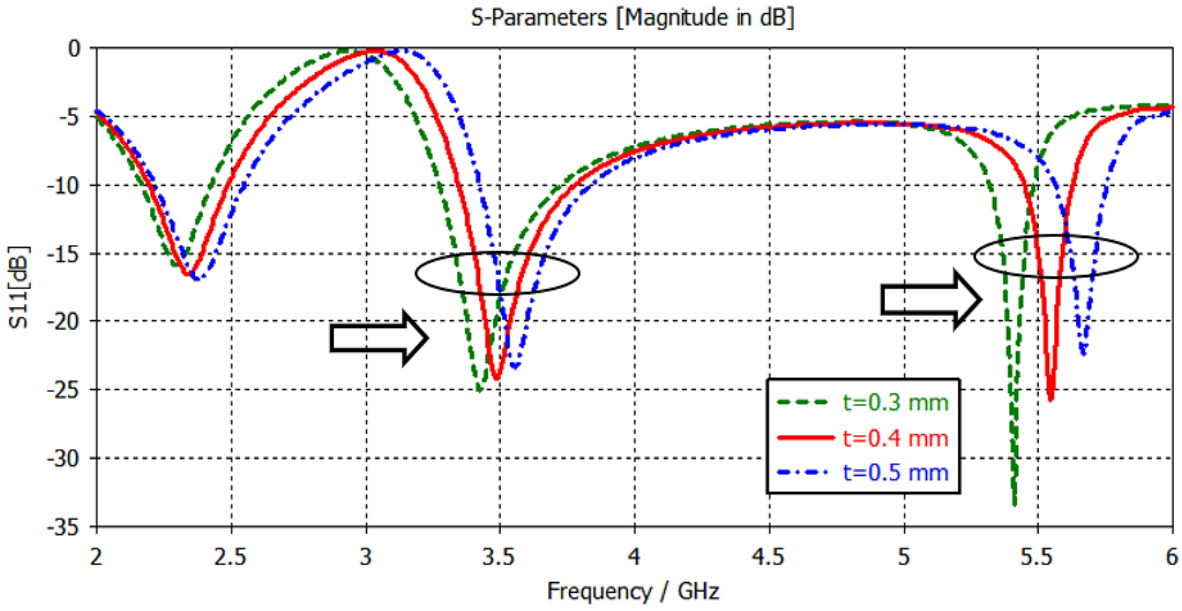

Figure 3. 6:The return loss of the proposed antenna, t is varying while R1 and g are kept constants.

3.4 Current distribution

Radiations from microstrip patch antenna can be determined from the field distribution between the patch metallization and ground plane. Alternatively, radiation can be described in term of surface current distribution on the patch metallization. The average current distributions are simulated at 2.34, 3.50 and 5.55 GHz as depicted Figure 3.6**.** It can be observed that, for the first resonant frequency, the current is mostly concentrated in the feedline and on the outer ring. Thus, the 2.34 GHz can be controlled by changing the radius Ro. For the second resonant frequency, the maximum

current concentration is seen over the strip line connection and the inner ring. Consequently, the 3.5 GHz can be controlled by tuning the gap g between the two rings, For the 5.55 GHz resonant frequency, it can be noticed that large concentration of current is recorded at the upper side of the outer ring and on the octagonal shaped branches .Hence , hole structure is involved in the radiation of the third frequency. However, fine tune of this resonant frequency can be controlled by changing the radius R1.

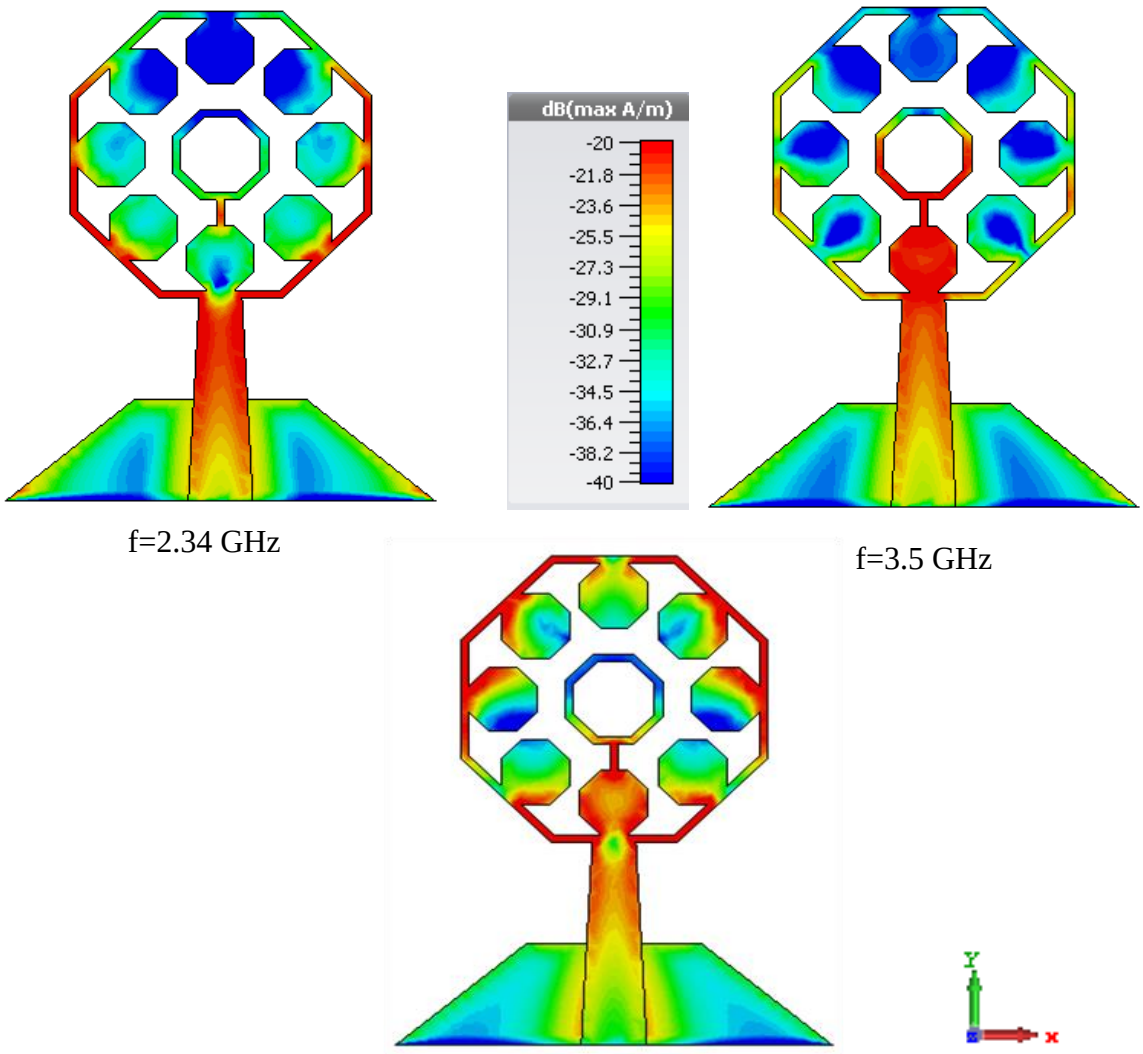

Figure 3. 7:Average current distributions of the proposed antenna at 2.34, 3.5 and 5.5 GHz.

3.5 Radiation pattern

The simulated radiation patterns of the proposed antenna at the resonant frequencies are represented in Figure 3.7. It can be seen that, at the first resonance frequency, the maximum gain is 1.82 dB and the antenna exhibits an omnidirectional radiation pattern in the H-Plane and dipole-like radiation in E-Plane. At the second resonance, similar radiation pattern as the first resonant frequency is observed with maximum gain of 1.91 dB. Omnidirectional radiation pattern in the H-Plane is observed at the third operating band while the slight deformation in the pattern occurs in the E-Plane.

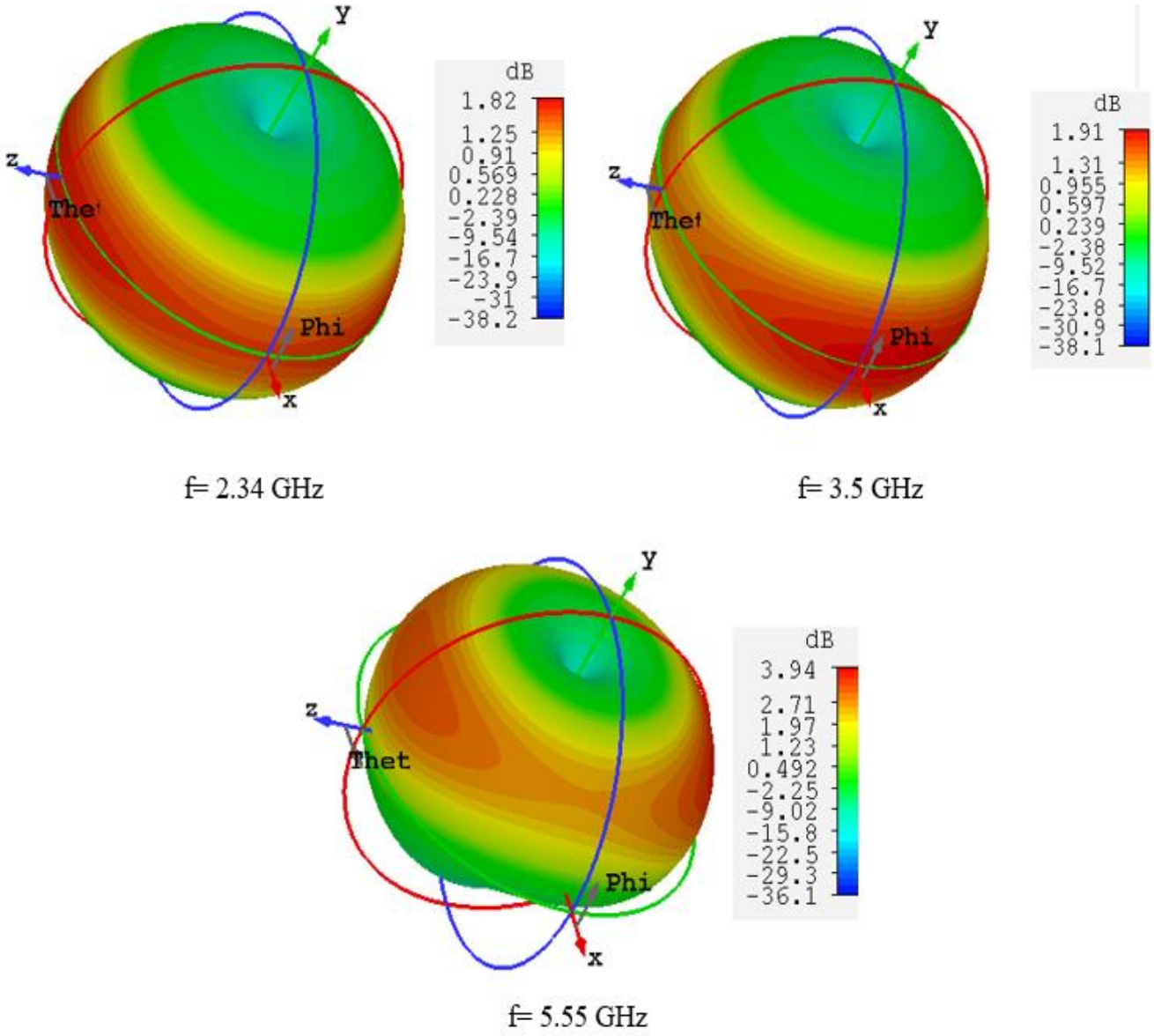

Figure 3. 8: 3D radiation patterns of the proposed antenna at different frequencies.

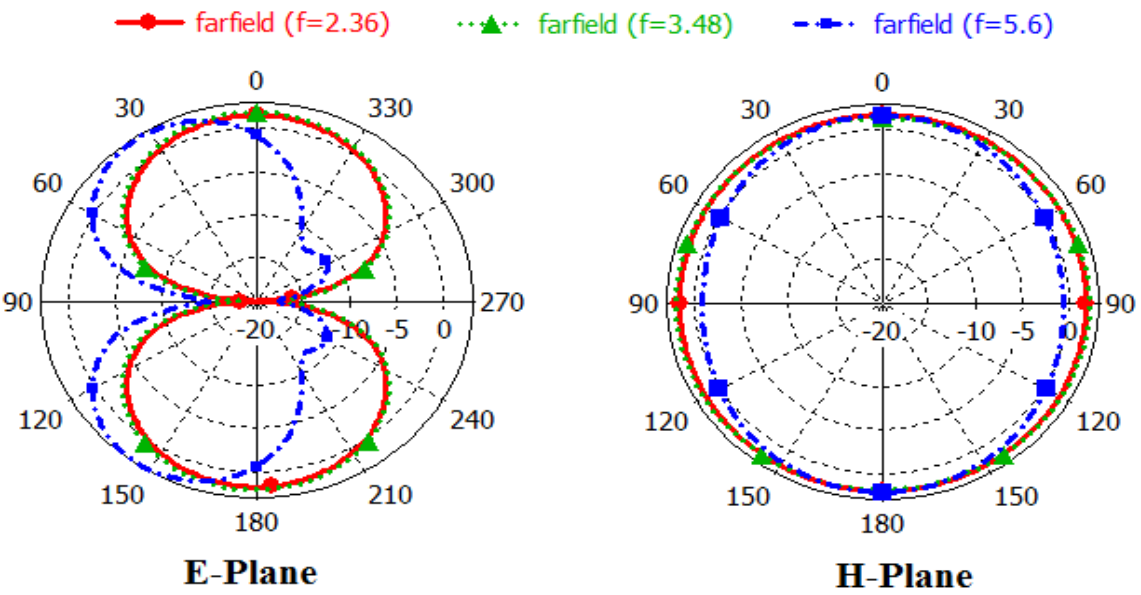

Figure 3. 9 :Radiation patterns of the proposed antenna different frequencies.

3.6 Fabrication and Measurement

The proposed tri-band monopole antenna is fabricated and tested. Figure 3.10 shows the photograph of the fabricated tri-band antenna. The fabricated antenna was measured using a vector network analyzer (VNA) available in the institute of Electrical and Electronic Engineering of Boumerdes University. The operating frequency range from 100 KHz to 20GHz (Figure 3.11). The measured and simulated return losses are shown in Figure 3.12**.** It can be observed that the simulated and measured results are in good agreement, showing a tri-band operation with measured 10-dB impedance bandwidths of 0.55 GHz (2–2.55GHz, 24.7%), 0.8GHz (3.40-4.2GHz, 22.2%) and 0.3GHz (5.40-5.70GHz, 5 %). The slight difference between the measured and simulated results may be due to the tolerance of fabrication unit and soldering of the SMA connector. The obtained bandwidths cover widely the WLAN and WiMAX applications which makes the proposed structure well suitable to be used in the intended application.

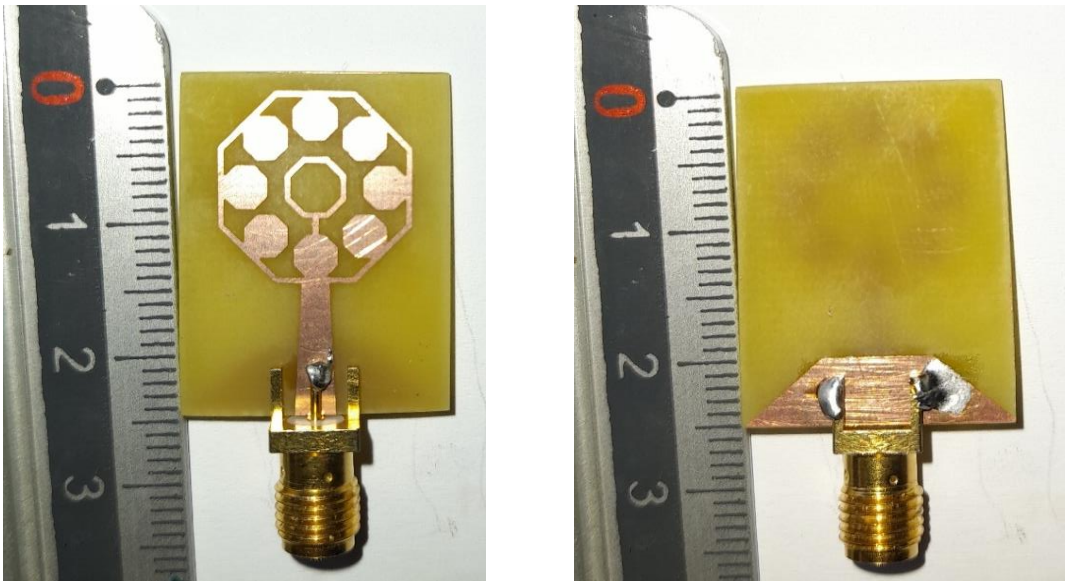

(a) (b)

Figure 3. 10:Photograph of the fabricated tri-band antenna prototype. (a) front view (b) back view.

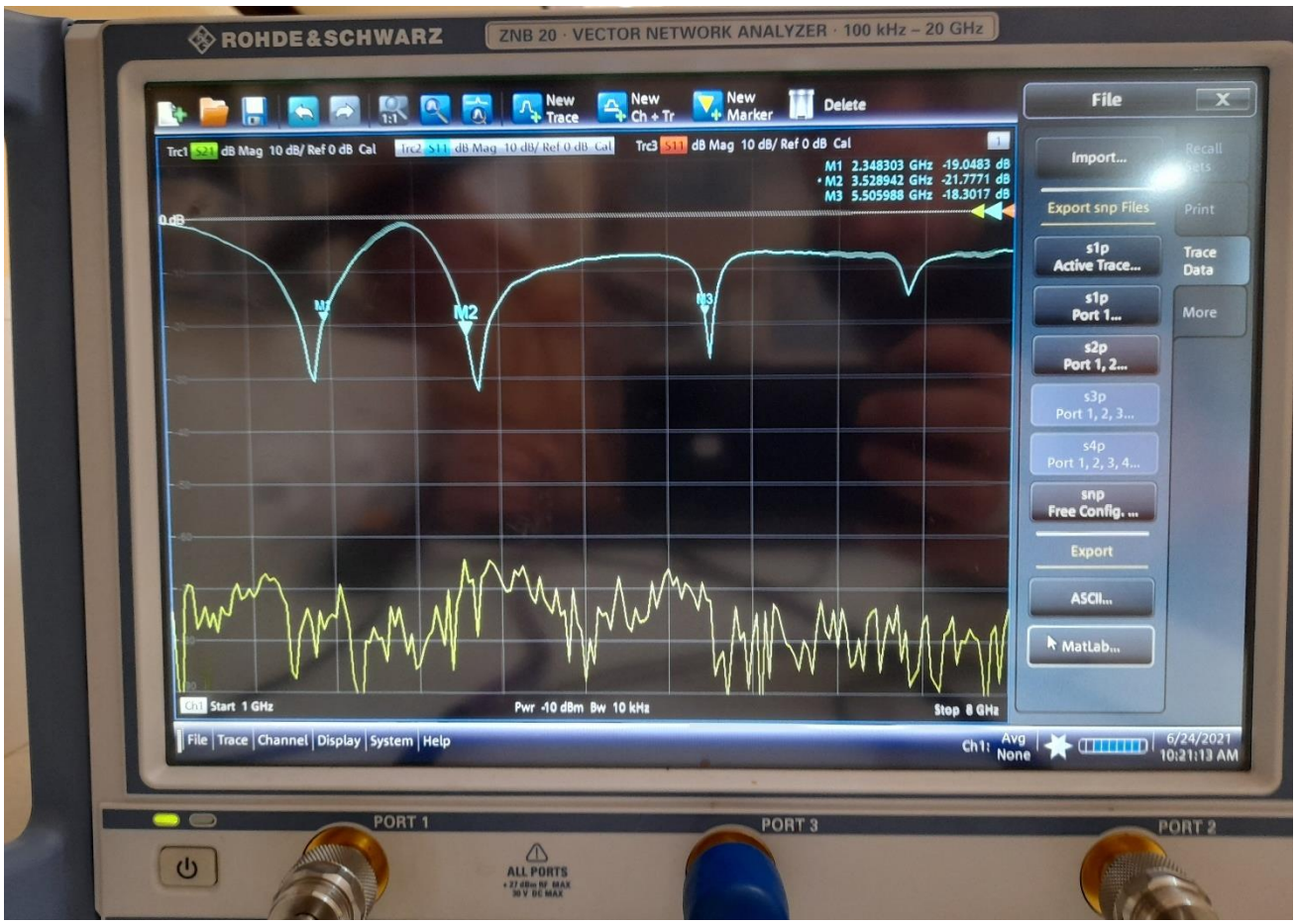

Figure 3. 11:The measured S11 displayed in the VNA screen.

A comparison between the proposed antennas and other antennas reported in the literature is presented in Table 3.12**.** By comparing the reported antennas footprints, it is clearly seen that the

proposed antennas have the smallest one. Consequently, it can be concluded that the proposed antenna achieves significant size reduction. Moreover, in terms of impedance matching performance, the proposed antennas outperform almost all the reported antennas.

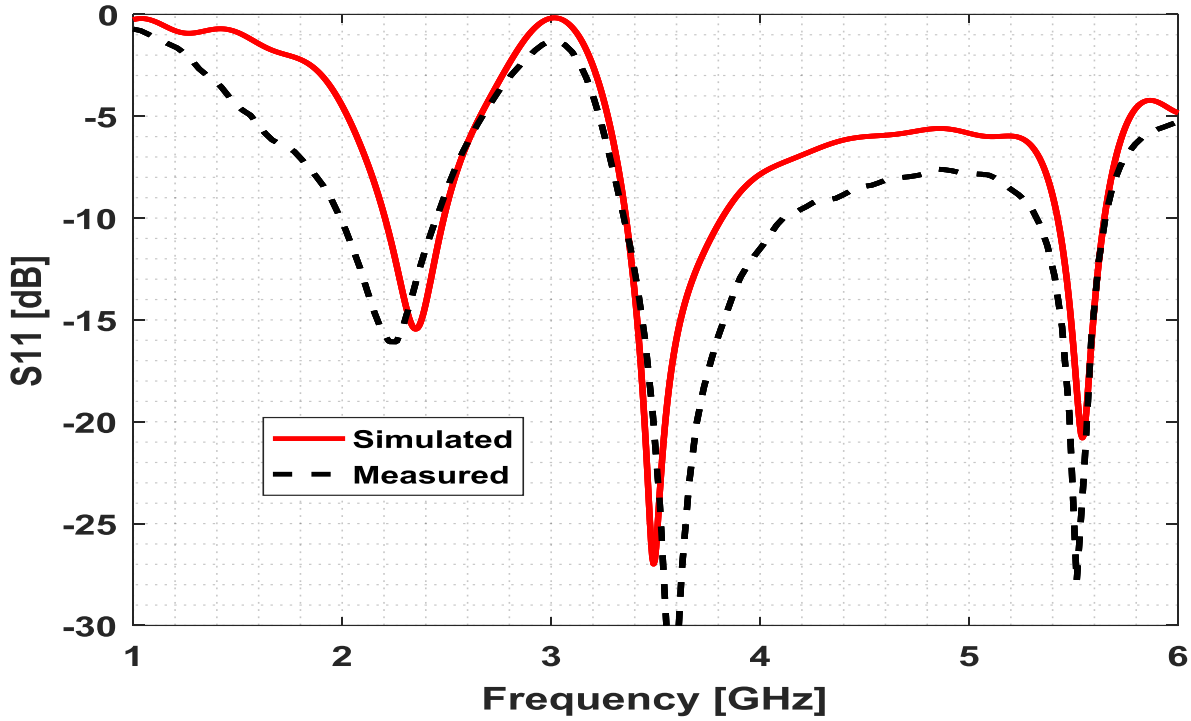

Figure 3. 12:Simulated and measured return losses of the proposed antenna.

Table.3. 2 :Comparison between proposed antenna size along with applications bands with others.

Reference	**Antenna Size (mm²)**	**Antenna Footprint**	**Operating bands**
[5]	23 ×20	0.027λ^2_0	2.39-2.52 GHz,3.3-4.47 GHz,5.15-6.0GHz
[6]	18 ×22	0.022 λ^2_0	2.27-2.50 GHz,3.28-3.81 GHz,4.91-5.98 GHz
[7]	35 × 38	0.048 λ^2_0	1.78-1.84 GHz,2.34-3.86 GHz,5.75-5.87GHz
[8]	18 × 18	0.022 λ^2_0	2.51-2.62 GHz,3.42-3.5 GHz,5.68-5.96GHz
[9]	32 × 12	0.026 λ^2_0	2.36-2.70 GHz, 3.35-2.74 GHz,5.01-6.12GHz
[10]	38 × 20	0.051 λ^2_0	2.32-2.51GHz, 3.05-3.95GHz, 5.4-5.85GHz
Proposed antenna	24×14	0.020 λ^2_0	2.21-2.49 GHz, 2.34-2.82 GHz 5.41-5.55 GHz

3.7 Size reduction

3.7.1 Patch size reduction

Figure 3.13 shows the geometry of two patches antenna, (a) the octagonal patch and (b) the proposed patch. The two antennas operate at 2.34 GHz, the size reduction is given as:

$$SR(\%) = \left(\frac{D_n^2 - D^2}{D_n^2}\right) \times 100 \tag{3.1}$$

$$SR(\%) = \left(1 - \frac{D^2}{D_n^2}\right) \times 100 \tag{3.2}$$

$$SR(\%) = 49.1\%$$

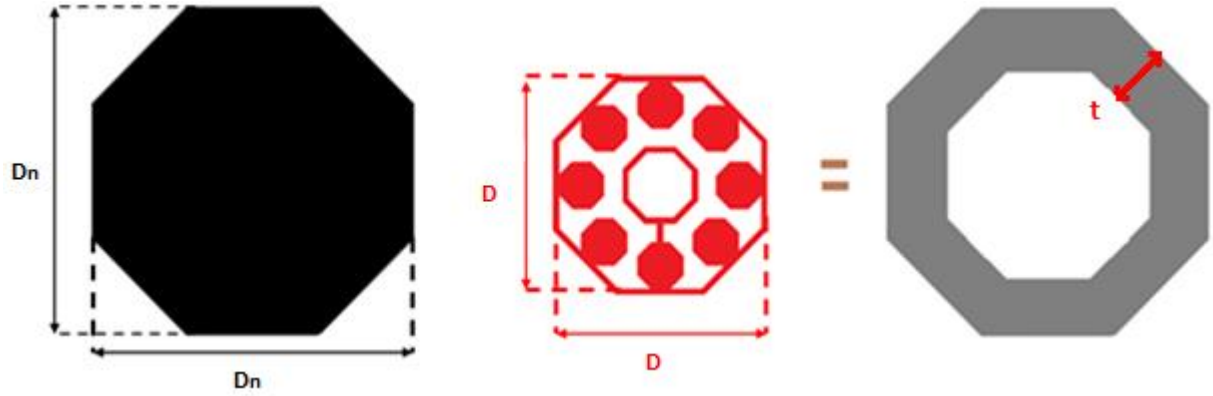

(a) (b)

Figure 3. 13: Comparison between the proposed patch and the octagonal patch .

3.7.2 Antenna size reduction

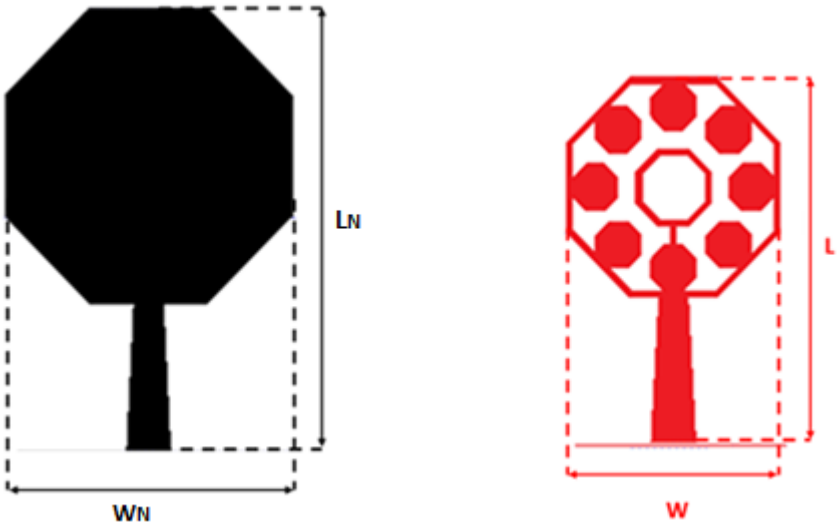

(a) (b)

Figure 3. 14:: Comparison between the proposed structure and the conventionnel octagonal patch antenna footprints.

Figure 3.14shows the proposed antenna and the conventional octagonal antenna operating at the same frequency of 2.34 GHz. It is clear from the figure that the proposed design occupies less area than the octagonal antenna. Moreover, the octagonal antenna is by itself a compact structure. The achieve size reduction is calculated using:

$$SR(\%) = \left(1 - \frac{W \times L}{W_N \times L_N}\right) \times 100 \tag{3.3}$$

$$SR(\%) = 44\%$$

3.8 Conclusion

In this chapter, a compact triple band antenna was designed, fabricated and tested. In the first part, the design procedure was detailed and a parametric study was performed in order to achieve an optimum design structure. In the last part, the proposed structure has been fabricated, tested and a good result in term of operating bands and compact size were obtained.

GENERAL CONCLUSION

In this work, a new compact tri-band microstrip antenna using two concentric octagonal rings has been proposed. The antenna geometrical configuration has been chosen carefully to operate in three commercially useful bands allotted to 2.4/5.5 WLAN and 3.5WiMAX applications.

Firstly, various shaped patches, having same radius, have been investigated. The octagonal shaped patch has been selected for its lower operating frequency and hence has minimum dimensions as compared to the investigated geometries including triangular, square, pentagonal, hexagonal and heptagonal.

Secondly, the octagonal structure has been loaded by an octagonal DMS slot to further reduce the antenna dimensions as well as achieve dual band operation under the frequency range extending from 2GHz to 7GHz. The resulted octagonal ring antenna return loss characteristics have been simulated and investigated through an extensive parametric study.

Then, a second octagonal ring has been loaded to the structure. The derived antenna is a dual-concentric interconnected octagonal rings monopole antenna. The number and the position of the connection strip, between the radiating rings, have been studied in details and it has been found that triple-band operation is achieved for one connection strip with and an adequate location. This intermediate structure covers the 2.4WLAN and 3.5 WiMAX bands. However, the third desired band 5.5WLAN band in not coved since the structure third operating band is centered at 6.53GHz extending from 6.18GHz to 7.27GHz.

In order to cover the 2.4WLAN, 3.5WiMAX and 5.5WLAN bands simultaneously, the outer radiating ring inner sides have been attached to eight octagonal shaped branches. The resulted structure which is the proposed antenna covers widely the intended bands. Furthermore, the proposed antenna operating frequencies are independently tunable to any desirable band by changing only one of its geometrical parameters. The proposed antenna has a compact size of only $L \times W = 24 \times 14\ mm^2$ and achieves **44%** size reduction as compared to the conventional octagonal shaped patch antenna.

References

[1] K. DJAFRI "Contribution to the Study and Design of Miniaturized Microstrip Antennas" .2018

[2] BALANIS, Constantine A. Antenna theory: analysis and design. John wiley & sons, 2015.

[3] Garg, R., Bhartia P, Bahl I., Ittipiboon A., "Microstrip Antenna Design Handbook", Artech House, Inc, 2001.

[4] AMERICAN RADIO RELAY LEAGUE. The ARRL antenna book. The League, 1949.

[5] ZAMAN, Wajid, AHMAD, Hamza, et MEHMOOD, Haris. A miniaturized meandered printed monopole antenna for triband applications. Microwave and Optical Technology Letters, 2018, vol. 60, no 5, p. 1265-1271.

[6] Vivek Kumar Pandit and AR Harish. A compact cpw-fed tapered monopole triple- band antenna for wlan/wimax application. Microwave and Optical Technology Letters, 60(9):2298-2303, 2018.

[7] Cheng Zhu, Tong Li, Ke Li, Zi-Jian Su, Xin Wang, Hui-Qing Zhai, Long Li, and Chang- Hong Liang. Electrically small metamaterial-inspired tri-band antenna with meta-mode. IEEE Antennas and Wireless Propagation Letters, 14:1738-1741, 2015.

[8] Tanweer Ali and Rajashekhar C Biradar. A triple-band highly miniaturized antenna for wimax/wlan applications. Microwave and Optical Technology Letters, 60(2):466-471, 2018.

[9] Le Kang, Hao Wang, Xin Huai Wang, and Xiaowei Shi. Compact acs-fed monopoleantenna with rectangular srrs for tri-band operation. Electronics Letters, 50(16):1112_1114, 2014.

[10] Xueshi Ren, Steven Gao, and Yingzeng Yin. Compact tri-band monopole antenna with hybrid strips for wlan/wimax applications. Microwave and Optical Technology Letters.